表3 グルコース負荷に対する血糖値およびインスリン分泌反応(雄仔ヒツジ22週齢)

	対照群*	低栄養群*
血糖ピーク(mM)	19.2±0.6	19.4±0
インスリンピーク(μM/m)	77.6±6.6	117.1±7.5

＊ブドウ糖の静脈内投与　0.4 g/体重 kg
(文献3より引用)

ている。このSinclairらの実験は，受精してわずか6日間だけであっても，メチル基を供与するone carbon metabolismに関与する栄養素が存在しない場合には，インプリント遺伝子のエピジェネティクス変化が生じることを明確に示すものである。やせた状態で妊娠する場合，果たしてこれら重要な栄養素を十分確保できているか否かは極めて疑問である。

人では分析可能な生体試料は限られており，報告は少ない。しかし少しずつであるが，人末梢血を試料として解析が行われている。オランダの飢餓事件に曝露されて生まれた人々の60歳前後での，末梢血リンパ球を対象として，インプリント遺伝子IGF-2・H19が分析されている(表4)[4]。Heijmansらは，末梢血有核細胞でインプリント遺伝子であるIGF-2のプロモーター域CpG(CpG1～CpG5)の，メチル化の解析をした。その結果，受精周辺期に低栄養に曝露された人々のみに，60歳現在でも，プロモーター域のCpGでは低メチル化がみられていた。ところが，それ以降に飢餓事件に曝露されて生まれた人々では，この低メチル化は生じていなかった。さらにインプリント遺伝子であるH19では曝露群でもその変化は認められなかった。すなわち受精周辺期の低栄養では一部のインプリント遺伝子にエピジェネティクス変化が起こり，それは一生存続していることがみられたのである。しかし同じ人々で，IL-10，レプチン，ATP-binding cassette A1，guanine nucleotide-binding protein，maternally expressed 3 (meg3)などのプロモーター域ではメチル化度が逆に亢進するという結果が示されている[5]。今なお，その全貌は不明であるといえるが，胎内低栄養の曝露は，各遺伝子ごとに異なったエピジェネティクス変化(主として低メチル化)を起こし，それが統合されて疾病は発症していくといえる。エピゲノムに影響する栄養素として，炭水化物，ビタミンA，ビタミンD，炭水化物，微量元素，さらにメチル基を供与する系(one carbon metabolism)に関与する葉酸，ビタミンB群などが挙げられている。それだけに

表4 オランダの飢餓事件で，受精周辺期に母親が低栄養に曝露されて妊娠した出生児のIGF-2遺伝子DMRのCpGメチル化度

	曝露群		対象群			
	(mean)	(SD)	(mean)	(SD)	差(%)	p(×10⁻⁴)
平均	0.488	(0.047)	0.515	(0.055)	−5.2	0.59
CpG1	0.436	(0.037)	0.47	(0.041)	−6.9	1.5
CpG2, 3	0.451	(0.033)	0.473	(0.055)	−4.7	41.0
CpG4	0.577	(0.114)	0.591	(0.112)	−2.3	4,100
CpG5	0.491	(0.061)	0.529	(0.068)	−7.2	14.0

DMR：differentially methylated region，オランダの飢餓事件当時のカロリー摂取量：400～800 kcal/day。
末梢血のIGF-2遺伝子のプロモーター域のCpG部位(1～5)のメチル化度を対照群と比較検討した。CpG4以外で有意差をもってメチル化が低下している。受精時の影響が出生後60年を経ても存続することが明らかとなった。このエピジェネティクス変化は時に世代を超えて存続する(Transgenerational effect)。
(文献4より引用)

受精周辺期の栄養の重要性は高い。

4．ヒツジでみた受精周辺期の低栄養と切迫早産

低栄養が切迫早産，早産を起こす可能性が指摘されている。それはヒツジを対象とした動物実験成果である[6]。人に適応できるか否かは不明であるが紹介する。ヒツジの妊娠期間は145～150日である。妊娠前60日から受精30日後まで母獣体重を15%減少させて飼育した(例えば体重60 kgの人では51 kgに減量)。その結果，対照ヒツジの妊娠期間は，146日に対し139日($p<0.05$)と短縮，すなわち早産が起こった(図5)。ヒツジの分娩発来はコルチゾールが高値となり，臓器の成熟が促されて生ずるとされている。そこで胎仔にカテーテルを留置してコルチゾール，ACTHを測定した。その結果，早産になった仔ヒツジでは，コルチゾールが早期に上昇が起こっている(cortisol surge)(図6)。

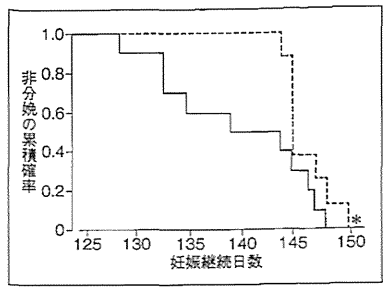

図5 妊娠前に母親ヒツジの体重を減少させた妊娠継続日数(Kaplan-Meier分析)
破線：対照群
実線：体重減少群　(文献6より引用)

またACTHの早期の増加があり，視床下部下垂体副腎皮質(HPA)軸の早期過剰反応が生じていることが明らかとなった。わずか妊娠初期30日間の体重減少を起こす低栄養曝露が，胎仔の内分泌系を大きく変化させたといえる。なお

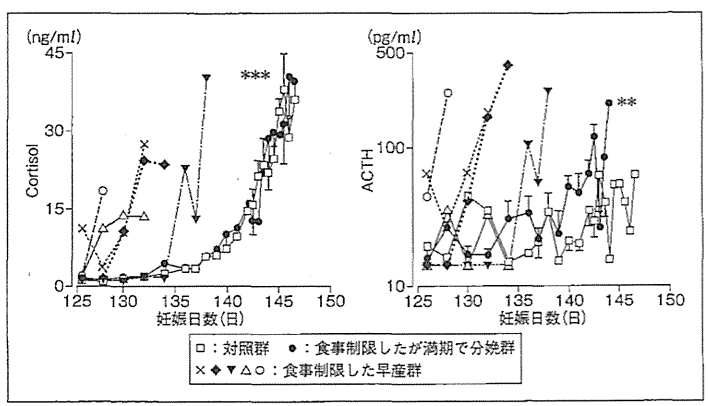

図6 妊娠初期に母獣へ低栄養曝露した胎仔ヒツジのCortisolとACTHの血漿濃度の推移
胎仔にカテーテルを留置して採血測定を行った。
***：$p=0.0001$，**：$p=0.01$，*：$p=0.05$(食事制限群 対 対照群)。
分娩予定日近くで分娩になった例では，胎仔コルチゾールが予定日に向けて少しずつ上昇しているが，早産例は早期にコルチゾールの上昇がみられて分娩に至っている。またACTH濃度は，満期分娩した例では一定の濃度で推移し，分娩日にかけて徐々に上昇している。しかし早産例は急激なACTHの上昇が認められている。受精前後の低栄養曝露は胎仔のHPA系の過剰反応が早期に生ずる状況の存在が示される。　(文献6より引用改変)

炎症性サイトカインが測定されているが炎症はみられておらず非炎症性に早産が生ずることを示した実験である。

おわりに

受精して生後1年間のわずかな期間(developmental stage)こそが，次世代の一生，あるいは世代を超えた健康あるいは疾病素因となるエピゲノム変化を大部分決定する時期である。しかも日本では第一子婚前妊娠が25～40%といわれており，若年時からの栄養の重要性を十分に理解して，自ら，および次世代への影響を考えて日常生活を送っていただきたいと切に願っている。今まで言われていた以上に，栄養が重要である。日々の栄養が，自分，家族，子ども，孫にまで影響することを理解して，日常の食生活を真剣に考えていただきたいことと，ダイエットの功罪も真剣に考えることが重要といえる。

文　献

1) Hanson MA, Gluckman PD : Early developmental conditioning of later health and disease : physiology or pathophysiology? Physiol Rev 94 : 1027-1076, 2014
2) Matusiak K et al : Periconception weight loss : common sense for mothers, but what about for babies? J Obes 20429, 2014
3) Sinclair KD et al : DNA methylation, insulin resistance, and blood pressure in offspring determined by maternal periconceptional B vitamin and methionine status. Proc Natl Acad Sci U S A 104 : 19351-19356, 2007
4) Heijmans BT et al : Persistent epigenetic differences associated with prenatal exposure to famine in humans. Proc Natl Acad Sci U S A 105 : 17046-17049, 2008
5) Tobi EW et al : DNA methylation signatures link prenatal famine exposure to growth and metabolism. Nat Commun 5 : 5592, 2014
6) Bloomfield FH et al : A periconceptional nutritional origin for noninfectious preterm birth. Science 300 : 606, 2003

妊娠高血圧症候群と母児の予後①

成人病胎児期発症説とPIHの胎児栄養
成人病胎児期発症起源説の視点から

福岡秀興*1　向井伸治*2

増加している成人病予防がこれからの医学の中心課題であり，「受精時や胎生期の子宮内および乳幼児期の望ましくない環境がエピゲノム変化を起こし，それが疾病素因となり，出生後のマイナス環境要因との相互作用によって成人病が発症する」という「成人病胎児期発症起源説」が注目されている。妊娠は一種の負荷試験であるゆえ，妊娠高血圧症候群(PIH)のリスク素因が胎生期に求められ，一部ハイリスク者のスクリーニングは妊娠した時点で可能と考えられる。PIHは胎児発育を障害するゆえに，児の予後改善を目的としたエピジェネティクスに関連した栄養学的介入により，児の疾病素因形成を阻止する視点からの治療が強力に行われるべきである。

はじめに

生活習慣病を含めた成人病が世界的に増えており，その発症予防がこれからの医学の中心課題である。生活習慣病や高リスクの疾患感受性遺伝子はその発症に関与しているが，それのみが主たる原因で疾患が発症するものではない。現在，「受精時や胎生期の子宮内および乳幼児期の望ましくない環境がエピゲノム変化を起こし，それが疾病素因となり，出生後のマイナス環境要因との相互作用によって成人病が発症する。成人病はこの2段階を経て発症する」という「成人病胎児期発症起源説」が発症機序として注目され，DOHaD(Developmental Origins of Health and Disease：的確な日本名称を日本DOHaD研究会で検討中)学説に発展・展開している[1]。出生体重は胎内環境を知る間接的マーカーであり，出生体重の低下は低栄養環境，環境化学物質，過大なストレスなどへの曝露によって，発育が抑制された状態であり，エピジェネティクス変化を介して成人病(生活習慣病)の発症リスクが高くなるといえる。また妊娠は疾病素因を有するか否かの負荷試験でもあり，高血圧素因がある場合には妊娠高血圧症候群(PIH)を発症しやすくなる。PIHは，胎児発育を障害する疾患であるがゆえに，その治療にあたりDOHaD説から母体と児の両者の予後改善を目的とした2つの視点を提示する。すなわちPIHの素因はPIH妊婦の胎生期環境に由来する考え方からのハイリスク者のスクリーニング，PIHを発症した母体に対し，エピジェネティクスからみた栄養学的検査を行い，栄養学的介入を行うことで，児の疾病素因形成を阻止するとの考え方である。そこで成人病胎児期発症説を概説し，その視点からのPIHハイリスク群の抽出の可能性についての一提言，PIH妊婦の栄養学的な管理の提言を述べたい。

1．成人病胎児期発症起源説

西欧では，古くより出生体重の低下と疾病罹患との関連について膨大な疫学研究が推進されてきたが，これはバーカー説，さらに発展してDOHaD学説として展開している[1]。また低体重児の有する疾病リスクの素因はエピジェネティクス変化である。これらの疾病群は，non communicative disease(NCD：WHO)とする新たな疾患概念でみられており，今後著しく増加していく。経済的発展が期待されている国で特に増加していく。胎生期，新生児期にその疾病素因が形成されるので，栄養状態が必ずしも良くない国が経済的な発展を遂げると著しいNCDが増加すると想定されている。疾病素因を有する妊婦に対し妊娠は一種の負荷試験であって，素因を有する場合その疾病が顕在化しやすい。出生体重が小さかった妊婦，すなわち子宮内で発育が抑制されて生まれた妊婦は生活習慣病の素因を有している可能性が高い。小さく生まれた妊婦は耐糖能低下の素因を有するので，妊娠糖尿病リスクが高く，高血圧でも同じく，出生体重の小さかった妊婦はPIHの発症リスクは高い。その背景や実際のコホート調査について，現在知られていることを述べる。

2．出生体重の低下と腎臓糸球体数の減少，高血圧発症

出生体重の小さい人は，高血圧を発症する例の多いことが知られている。しかし若年時には，小さく生まれていても対照群に比べ血圧に差はみられていない。ところが35歳を過ぎると血圧の差は顕在化していく。高血圧素因を有していても生体は血圧に対して相当に強い予備能が備わっていると想像される。出生体重の小さい場合は，腎臓糸球体の数が少ない。そこで糸球体数の減少こそが本態性高血圧症の原因であるとする「ブレンナー説」が提案されている。Barry M. Brennerによる，「本態性高血圧は，腎臓糸球体・ネフロン数の減少により生ずる。それは望ましくない胎生期子宮内環境(低栄養，ストレス，化学物質曝露)，遺伝子要因，早産で生ずる。低ネフロン数状態は腎臓糸球体の肥大を起こし，やがて高血圧，CKD，腎硬化症，腎不全を発症するに至る」という説(1989年)である[2]。

現在まで小児の剖検例で，腎臓糸球体数を組織学的に検討した13前後の報告ではすべて，出生体重の低下は腎臓糸球体数の低下を伴うとされている。キューバからの報告[3]を提示するが，出生体重が3,000 g以下になると，腎臓糸球体数の低下が認められ，腎臓糸球体数と腎臓糸球体体積とは逆相関を示している(図1)[3]。腎臓糸球体数が少なくなると，代償的に腎臓糸球体が肥大して代償しているのである(compensatory glomerulomegaly and hyperfiltration現象)。腎臓は，妊娠8週頃から34～36週で組織形成が起こる。その2/3は妊娠末期に完成し，出生後は腎臓糸球体の形成は行われない。それゆえ出生時に腎臓糸球体数が少なければ，一生を通じて個々の腎臓糸球体には大きな負荷がかかり続けることとなる。出生時からすでに，リスクを追って一生を過ごさねばならなくなる。DJ Barkerが，バーカー説を提示した頃でもあり，英国・米国で同時期に，劣悪な胎生期環境では成人病素因が形成される現象に注目したのは興味深い。30年を経過した現在，代謝性疾患の発症素因は胎生期のエピジェネティクス変化にあることが明らかになりつつあり，生命科学の着実な進歩が窺われる。

交通事故で死亡した男性(36～58歳)の剖検例で，本態性高血圧と正常血圧群に分けて腎臓糸球体数を比較したところ，高血圧群では明らかな腎臓糸球体数の低下があった。また腎臓糸球体の体積は数の減少とともに増加していた(図2)[4]。詳細な検討で，出生後に腎臓糸球体が消失，減少した所見は認められず，出生時にすでに数が少なかった可能性が高いとの見解が示されており，ブレンナー説を傍証する成果として世界的に注目された報告であった。

3．出生体重低下とPIH発症

妊娠糖尿病と同じく妊娠は一種の負荷試験であり，高血圧を発症する素因があると，妊娠により高血圧が発症するリスクが高い。出生体重とPIHの発症リスクを検討した有名なSeattle and Tacomaスタディ(1998～2001)があるので紹介する(表1)[5]。年齢，人種，経産回数，教育

*1　Hideoki Fukuoka　早稲田大学総合研究機構
*2　Shinji Mukai　国立病院機構高知医療センター臨床検査科

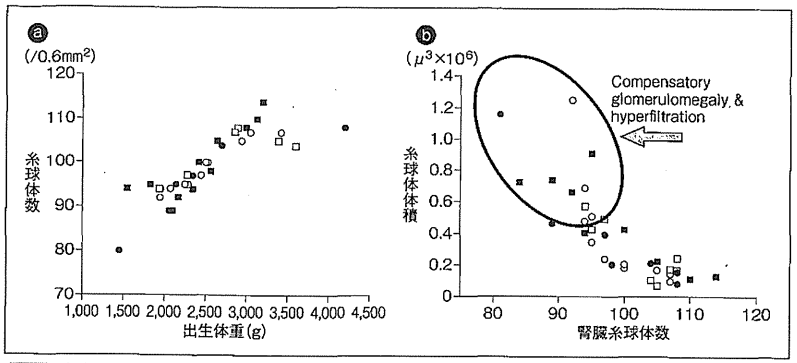

図1 出生体重と腎臓糸球体数および体積
小児剖検例での出生体重と腎臓糸球体数の相関性と腎臓糸球体数と糸球体体積の相関性をみたもの。出生体重が3,000 g以下になると直線状に腎臓糸球体数が低下している。糸球体数の低下は，1つの糸球体への負荷が大きくなり代償性に肥大している。これはやがて腎硬化症，腎不全に発展する。
(文献3より引用改変)

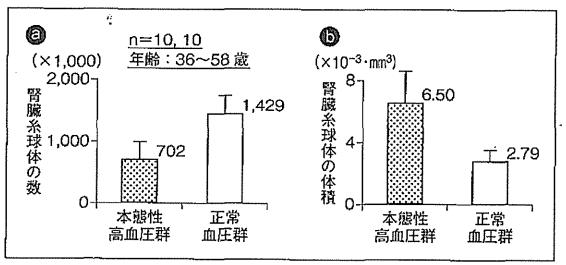

図2 本態性高血圧者の腎臓糸球体の数と体積
交通事故で死亡した男性(36～58歳)で，本態性高血圧症のある例とない例それぞれ10例の剖検で，腎臓糸球体数及び体積をみたもの。両群では明らかに腎臓糸球体数，体積に差が存在している。胎生期の影響が後年血圧に影響する機構を示すものといえる。
(文献4より引用改変)

歴，18歳のBMIで補正して検討したものである。その結果，2,500 g未満での出生群は，2,500～3,000 g未満の出生体重群に比べ，オッズ比2.27(95%CI：0.97-5.27)とリスクが高い。出生体重が3,000～3,999 gと大きくなると，オッズ比0.56(95%CI：0.39-0.94)と低下している。しかし4,000 g以上では糖尿病のリスクを有する群が混じってくると思われる。この成績は妊娠が疾病素因に対する明確な負荷試験であることを示している。それゆえ，PIHを発症した母親は，高血圧素因を有するので，母親の予後を改善するためには早期介入・早期治療が必要である。分娩後の生活習慣，早期の治療を含めたケアの重要性を母親にしっかりと自覚してもらい，経過観察していく必要がある。それは産科医の大事な責務といえる。妊娠糖尿病患者に対する指導と同じである。

肥満はPIHの需要なリスク因子である。そこで，さらに妊娠した時点での肥満度と出生体重との関連が検討された(表2)[5]。2,500 g未満で生まれ，妊娠時BMI 25以上の肥満群では，2,500 g以上で生まれ，BMI 25以下の非肥満群に比べ補正オッズ比は，23.85(95%CI：5.91-96.27)という極めて高いリスクを示している。小さく生まれて体重を増やした妊婦は，疾病発症リスクが著しく高くなることが伺われる。ところが2,500 g以上で生まれた場合でも，肥満状態で妊娠した場合は，オッズ比5.88(95%CI：3.44-10.03)と高いリスクを示している。肥満自体が1つのリスク因子である。ひるがえって，小さく生まれた場合でも，妊娠時に肥満でない場合は，オッズ比2.04(95%CI：0.78-5.36)とリスクは高いが，肥満して妊娠した場合に比べて，そのリスクは随分と低い。出生体重の低下は，高血圧を発症するリスクが高いといえる。出生体重の低下は腎臓糸球体数の低下を伴うので(図1)，この疫学調査もブレンナー説を傍証するものと考えられる。

以上の結果は今後，妊婦の初診時には出生体重，妊娠期間，妊娠合併症の有無のチェックがPIHのスクリーニング上必須の事項となるべきであることを示している。それにより妊娠中の管理の個別化が可能と期待される。

4．腎臓糸球体数の減少機構

胎内の低栄養曝露による腎臓糸球体数の減少機序は，なお明確でないが，PIHでは，低栄養，過剰なストレスなどが胎児に負荷され，レニンアンギオテンシン系〔(Renin-Angiotensinsystem；RAS)系〕の抑制，過剰なストレス負荷によるグルココルチコイドへの過剰な曝露，アポトーシスの亢進という3つの機序が想定されて，腎臓糸球体数の減少が起こる。

1 RAS系の抑制

アンギオテンシンⅡ受容体にはAT1，AT2の2種が存在している。ラットは生後1週間は腎臓糸球体の形成が行われるので，出生仔ラットに1週間，それぞれの受容体阻害剤であるロサルタン，PD123319を投与したところ，AT1阻害剤により，著しい体重抑制，腎臓重量の低下，DNA合成の抑制がみられた。そのため長く，AT1受容体を介して腎臓糸球体が形成されるとされてきたが，その後，AT2受容体を介するPax-2の系が腎臓糸球体形成に関連していることが明らかにされた。また胎内の低栄養環境は，AT1，AT2の発現，特にAT2発現が強く抑制されることが明らかとなった[6]。さらに，腎臓組織の形成(nephrogenesis)過程，特に腎臓糸球体の形成に重要な関与をしている因子であるPax-2の発現は，AT2を介して促進される。それゆえ，胎内の低栄養環境ではAT1，AT2を含めたRAS系(特にAT2)の発現が抑制されて，腎臓糸球体形成が抑制されると考えられている。

2 過剰なグルココルチコイドへの曝露

低蛋白質食を妊娠母獣ラットに投与することで，組織では多様な変化が起こる。特に，胎盤

表1 出生体重と妊娠高血圧症候群のリスク(シアトル・タコマスタディ)

出生体重(g)	オッズ比*	(95%CI)
<2,500	2.27	(0.97～5.32)
2,500～2,999	1.00	Ref.
3,000～3,999	0.56	(0.34～0.94)
4,000<	0.46	(0.17～1.21)

*：年齢，人種，経産回数，教育歴，18歳のBMIで補正。 (文献5より引用)
(Seattle and Tacoma study, in Washington, 1998～2001)

表2 出生体重と妊娠前BMIからみた妊娠高血圧症候群リスク

出生体重	妊娠前BMI	オッズ比*	(95%CI)
<2,500 g	25<	23.85	(5.91～96.27)
	<25	2.04	(0.78～5.36)
2,500 g<	25<	5.88	(3.44～10.03)
	<25	1	Ref.

*：年齢，人種，経産回数，教育歴，18歳のBMIで補正。 (文献5より引用)
(Seattle and Tacoma study, in Washington, 1998～2001)

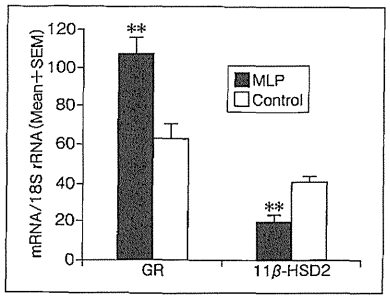

図3 ラット母獣への低蛋白食投与による出生仔腎臓のGR, 11βHSD2遺伝子発現

妊娠ラットに低蛋白食を負荷して，出生仔の腎臓のGR(グルココルチコイド受容体)と11βHSD2(11βhydoroxysteroid dehydrogenase type 2)の遺伝子発現の比較を行ったもの。低蛋白質食の負荷でGRの過剰発現，11βHSD2の低発現がみられる。仔には過剰なグルココルチコイドに曝露される状況が生じている。(文献7より引用改変)

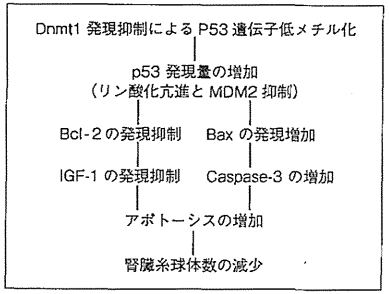

図4 アポトーシスによる腎臓糸球体減少の一機序

のグルココルチコイド非活性化酵素の11β HSD2(11β hydroxysteroid dehydrogenase type Ⅱ)の発現が抑制され，腎臓の11βHSD2の発現抑制とグルココルチコイド受容体(GR)の発現が亢進する(図3)[7]。この変化はエピジェネティクスの変化(11βHSD2のプロモーター域の高メチル化，GRプロモーター域の低メチル化)によるものである。グルココルチコイド非活性化の抑制と，グルココルチコイド受容体の増加が起こるこの腎臓での変化は，血中のグルココルチコイド濃度が同じであったとしても，組織には，より多くのグルココルチコイドが作用することを意味する。組織が過量なグルココルチコイドに曝露されることで，腎臓ではRAS系に関連した遺伝子発現が抑制される。特にAT2を介するPax-2発現が抑制されて，腎臓糸球体形成が抑制されることとなる。早産ではRDSの予防に母体にグルココルチコイドを投与して，胎児肺胞の成熟を促す治療が行われる。胎盤には11βHSD2が存在しているために，酵素の基質でないデキサメサゾンなどが投与されるが，投与量が多いと，出生体重の低下，腎臓重量の低下，高血圧，蛋白尿，組織のNa含量の増加などが生ずる。腎臓糸球体数の減少も生ずる。

3 アポトーシスの亢進

アポトーシスの1つの経路として図4がある。Phanらは，妊娠ラットで妊娠19日に子宮動脈結札による強い胎内低栄養環境を作り，腎臓でのアポトーシスの亢進と腎臓糸球体数の減少の生ずることを確認して，その機序を検討した[8]。概略，まずDNAにメチル基を結合させる酵素(DNA methyl transferase 1)の酵素活性の低下が起こり，その結果，p53遺伝子の低メチル化が生じて過剰発現する。p53の過剰発現により，細胞増殖因子であるBcl-2，IGF-1の発現が抑制され，同時にアポトーシスを起こすBax，Casparse-3の発現が増加する。この2つの現象により，アポトーシスが著しく亢進する。その結果，出成されていた腎臓糸球体にアポトーシスが起こり腎臓糸球体の減少が生じてきたのである。

5．人胎内低栄養とエピジェネティクス

胎内低栄養を負荷する動物実験で，脂質代謝，交感神経系，視床下部-下垂体-副腎系，海馬，腎臓などでのエピゲノム変化の解析が進んでいる。しかし同じ疾病(同じ表現型)が発症しても，動物種によりその原因としてのエピゲノム変化は異なっていることが指摘されている。同じ疾病でも，種によりエピゲノムの変化は異

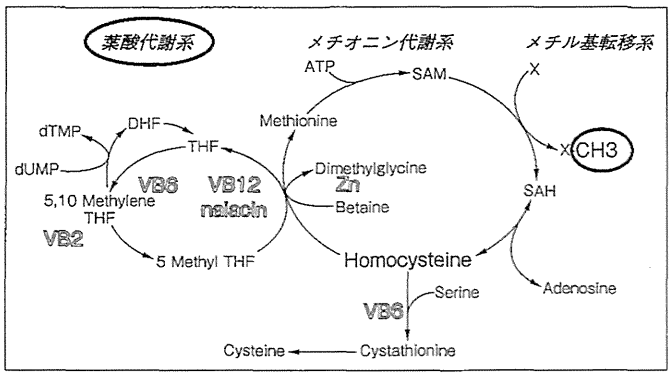

図5 遺伝子の機能を調節するメチル基の代謝(One carbon metabolism)

葉酸から始まるこの代謝系で最終的にメチル基が形成されエピジェネティクスを制御する。この代謝回転がスムーズに動かない場合にホモシステインが高値となる。

なっているので，人の疾病発症機構の解明には，人での解析が必要である。人で分析できる生体資料は，手術以外では，血液，胎盤，臍帯と限定されており，解析が難しい。しかし，その分析が進んできた。臍帯血Hcyが高値の場合Line1遺伝子の低メチル化の起こる現象，臍帯のRXRα遺伝子，「オランダの冬の飢餓事件」に曝露された人の末梢血で，インプリント遺伝子であるIGF-2などでのエピゲノム変化が解析されている。

メチル基がDNA，ヒストンに結合することによりエピジェネティクスが変化する。エピジェネティクスの代謝系の1つとして，メチル基がDNAまたはヒストン蛋白に結合する経路(one carbon metabolism)があり，その代謝経路は葉酸から始まる。それにビタミンB2, B12, メチオニン，グリシン，亜鉛などがその代謝に関与する酵素に補酵素として作用して，最終的にはs-adenosyl methionine(SAM)が形成されてメチル基が供与され，エピゲノム変化が起こる(図5)。この代謝系では，葉酸に加えてこれら栄養素の必要で十分な量が存在することが，スムーズな代謝回転に必要である。これら多様な栄養素が妊娠中に特に必要である。そうでない場合には，望ましくないエピジェネティクスの変化が起こる。その指標として中間代謝産物としてのホモシステイン(Hcy)がある。高値は代謝回転の異常が想定される。Anthonyら[9]は臍帯血で血中ホモシステインとLine1遺伝子プロモーター域のメチル化の程度を検討し，Hcy濃度が上昇するとメチル化度の低下が認められるとした。この分析はLine 1遺伝子にのみ注目されているが，他の遺伝子にも同様の変化が生じている可能性がある。このように母体の葉酸および他の栄養素の濃度は，児のエピジェネティクスを変える可能性を示唆する知見が得られつつある。PIHは胎児発育が抑制される場合が多く，one carbon metabolismに関連した栄養素は特に考慮すべきといえる。

6．One carbon metabolismからみた妊婦栄養

PIHは，児の発育が抑制されるのでエピジェネティクス変化が生じている。それゆえ特にエピジェネティクスに影響する栄養素を測定し，不足した栄養素は速やかに補充していくことが行われれば，たとえ出生体重が小さくても成人病の発症リスクは大きく抑制される。PIHの次世代への連鎖を断つためにもその視点からの臨

床が行われるべきである。

1 葉　酸

葉酸は，妊娠中には，神経管閉鎖障害の予防に加えて，母体や胎児の細胞分裂の増加，胎児の葉酸の必要量の増加や葉酸代謝速度の亢進により，葉酸必要量が著しく増加する重要な栄養素である。葉酸は，one carbon metabolismsのスタートとなる物質であり，プリン・ピリミジンを形成してヌクレオチド合成に代謝される系と，s-adenosylmethionine(SAM)を形成して，メチル基の供与系として，エピジェネティックスの代謝および神経伝達物質などの形成系を構成しており，全妊娠中を通じて，重要な栄養素である。図5にこの代謝系を示す。この代謝に関与する酵素は多数存在し，多くの栄養素が補酵素として機能しており，葉酸や多様な栄養素が児のエピジェネティックス代謝に関与している。それゆえにPIHでは，特にこの代謝系における中間代謝産物，補酵素として機能する栄養素の測定が行われ，その不足・異常な高値の有無を検討するべきである。不足した栄養素は，食事あるいはサプリメントにより速やかに補充していくべきである。

葉酸は妊娠前から妊娠期間中は，サプリメントによる必要量を摂取し続ける必要がある。ところが，妊娠中期以降の葉酸の過量摂取は喘息を発症するリスクがあるとする報告が公表されてから，中期以降の摂取量は激減しており，葉酸の不足した妊婦が多い。もし母体の葉酸濃度が低いと，胎児での不足が起こり，それは胎児にエピゲノム変化が生ずる可能性があり，それが危惧されている。全妊娠期間中，過量摂取と摂取不足は厳に慎むべきである。

2 高ホモシステイン血症とビタミンB群

図5に示すように，葉酸濃度が低いと，one carbon metabolismの代謝回転がスムーズに進まず，中間代謝産物であるホモシステイン濃度は上昇する。非妊娠時に若年でもホモシシテインが高値であると，動脈硬化を起こすことがある。またフラミンガムスタディでもHcyの高値は多様な成人病の発症と関連づけられている。同様に妊娠中のHcy高値は多くの妊娠合併症を起こすので，Hcyの高値は何としても避けなくてはならない。例えば，大規模なノルウェーでの妊婦の調査[10]では，四分位値で最上位の女性は最下位の女性と比較して，PIH発症リスクは32%，早産児の出産リスクは38%，さらに極低出生体重児の出産リスクは101%高いと報告されている。また胎盤早期剝離は，血漿ホモシステイン濃度が高い母親で発症頻度は高い傾向にあった。スペインでの研究[11]では，妊娠前および妊娠中の母体血中のホモシステイン濃度と臍帯血ホモシシテイン濃度とは相関しており，高値例では出生体重は低くなる傾向が認められている。妊娠2カ月時と出産時の血漿ホモシステイン濃度が三分位値で最上位の母親では，最下位三分位の群に比べ，低出生体重児のリスクは，やはり高いと報告されている。

これらの結果は，one carbon metabolismの代謝をみると，葉酸欠乏のみでHcyが高値になるものでないことは理解できる。すなわち，葉酸に加えて，リボフラビン，ビタミンB6，ビタミンB12，亜鉛が欠乏しても，血漿Hcyが高まるのである。そこで高Hcy血症に対する治療には，one carbon metabolsimに関連して不足している栄養素の食事あるいはサプリメントによる速やかな補充が必要である。妊娠中のこれら栄養素を摂取する重要性を葉酸と同位置に考えることが必要である。

PIHの発症時には，母体の管理に加え，胎児の栄養の管理，特にエピジェネティクスに影響する栄養素の投与を，全妊娠期間を通じて積極的に行う必要がある。ただし，注意すべき点は，葉酸サプリメントの過剰な摂取については十分な配慮が行われなくてはならないことである。One carbon metabolismに関与する酵素遺伝子多型がない場合は，1,000 μg以上の葉酸は児に，アレルギー性疾患や代謝性疾患を起こす可能性がある。

7．ミネラル類，カルシウム

妊娠中は消化管からのカルシウム吸収量が著しく高まり，経胎盤的にCaは能動輸送される。合併症のない場合に，胎盤・羊膜で大量の1α25(OH)2Dが産生され，母体の消化管からのCa吸収率を高めていることによる。それゆえ妊娠合併症のない妊婦では，推奨量以上のカルシウム摂取は必要がない。ところが，PIHでは，胎児付属物での1α25(OH)2D産生は抑制されており，Ca吸収量は少なく，母体のCa不足があり，Ca不足による血圧の上昇も生じると考えられるので，PIHの場合はCaの摂取量を多くすべきである。

妊娠高血圧症候群では，Caの多量摂取が血圧を低くするとの疫学的および実験的な報告がある。PIH例では確かに血圧をコントロールする効果がみられている。そこでCaがPIHの発症リスクを減少させうるか否かに関する調査が行われた。Ca摂取量の低い値域で行われた無作為化二重盲検試験では，375～2,000 mgのカルシウム補給を行うと，母体の血圧をかなり下げたとされる。反対に，米国での4,589人の妊娠女性を対象とした多施設共同カルシウム投与介入試験では2,000 me/日のカルシウムサプリメントを投与しても，PIHの発症リスクへは影響しないとの結果であった[12]。カルシウムを多く摂取していても，Ca摂取量が平均422 mgと少なくても，発症リスクを下げるものではなかった。

以上より，PIHが発症していない場合は目安量600～700 mgを摂取すればよく，従来いわれてきたように妊娠中にそれ以上を摂取する必要はない。しかしPIHを発症した場合は，より多くのCa摂取を心掛けるべきであり，血圧にも良い影響を与える。なおカルシウムに関連し，ビタミンDとセレンの不足した妊婦では，PIH発症リスクが高いので，これらの予防的投与も今後検討されるべきである。

おわりに

PIHは特に児のエピジェネティクス変化を生じやすい疾患であり，それだけに，より栄養学的な管理を行うことこそが，積極的に行われるべきである。出生体重の低下が進行している日本では，妊娠前の痩せ，妊娠中の体重増加抑制，「小さく産んで大きく育てる」ことがよいとする風潮など，必ずしも胎児の発育に望ましくない状況があり，健やかな次世代を送りだすべき周産期医療関係者の責務は大きいといえる。

文　献

1) Hanson M, Gluckman P : Developmental origins of noncommunicable disease : population and public health implications. Am J Clin Nutr 94(6 Suppl) : 1754S-1758S, 2011
2) Brenner BM et al : Glomeruli and blood pressure : Less of one, more the other? Am J Hypertens 1 : 335-347, 1988
3) Mañalich R et al : Relationship between weight at birth and the number and size of renal glomeruli in humans : a histomorphometric study. Kidney Int 58 : 770-703, 2000
4) Keller G et al : Nephron number in patients with primary hypertension. N Engl J Med 348 : 101-108, 2003
5) Dempsey JC et al : Weight at birth and subsequent risk of preeclampsia as an adult. Am J Obstet Gynecol 189 : 494-500, 2003
6) Zhang SL et al : AngiotensinⅡ increases Pax-2 expression in fetal kidney cells via the AT2 receptor. J Am Soc Nephrol 15 : 1452-1465, 2004
7) Bertram C et al : The maternal diet during pregnancy programs altered expression of the glucocorticoid receptor and type 2 11beta-hydroxysteroid dehydrogenase : potential molecular mechanisms underlying the programming of hypertension in utero. Endocrinology 142 : 2841-2853, 2001
8) Pham TD et al : Uteroplacental insufficiency increases apoptosis and alters p53 gene methylation in the fullterm IUGR rat kidney. Am J Physiol Regul Integr Comp Physiol 285 : R962-970, 2003
9) Fryer AA et al : LINE-1 DNA methylation is inversely correlated with cord plasma homocysteine in man : a preliminary study. Epigenetics 4 : 394-398, 2009
10) El-Khairy L et al : Plasma total cysteine, pregnancy complications, and adverse pregnancy outcomes : the Hordaland Homocysteine Study. Am J Clin Nutr 77 : 467-472, 2003
11) Murphy MM, Fernandez-Ballart JD : Homocysteine in pregnancy. Adv Clin Chem 53 : 105-137, 2011
12) Belizán JM et al : Calcium supplementation to prevent hypertensive disorders of pregnancy. N Engl J Med 325 : 1399-1405, 1991

Accurate Prediction of the Stage of Histological Chorioamnionitis before Delivery by Amniotic Fluid IL-8 Level

Satoshi Yoneda[1], Arihiro Shiozaki[1], Mika Ito[1], Noriko Yoneda[1], Kumiko Inada[1], Rika Yonezawa[1], Mika Kigawa[2], Shigeru Saito[1]

[1]Department of Obstetrics and Gynecology, University of Toyama, Toyama, Japan;
[2]Department of Public Health Faculty of Medicine, University of Toyama, Toyama, Japan

Keywords
Amniotic fluid, body temperature, histological chorioamnionitis, interleukin-8, preterm labor

Correspondence
Shigeru Saito, Department of Obstetrics and Gynecology, University of Toyama, 2630 Sugitani, Toyama, 930-0194, Japan.
E-mail: s30saito@med.u-toyama.ac.jp

Submission December 4, 2014;
accepted January 2, 2015.

Citation
Yoneda S, Shiozaki A, Ito M, Yoneda N, Inada K, Yonezawa R, Kigawa M, Saito S. Accurate prediction of the stage of histological chorioamnionitis before delivery by amniotic fluid IL-8 level. Am J Reprod Immunol 2015

doi:10.1111/aji.12360

Objective
To estimate the stage of histological chorioamnionitis (h-CAM) antenatally using clinical data.

Materials and methods
Four hundred and twenty-eight singleton mothers were recruited. Clinical data including the levels of white blood cell count (WBC), C-reactive protein (CRP), amniotic fluid interleukin-8 (AF-IL-8) at Cesarean section, and maternal body temperature (MBT) were collected.

Results
Histological chorioamnionitis was present in 45.3% of the cases. Poor neonatal prognosis was highest (59.1%) in cases with h-CAM stage III. AF-IL-8 (odds ratio: 8.5, 95% CI: 5.1-14.8, $P < 0.0001$) and MBT (odds ratio: 2.3, 95% CI: 1.13–4.1, $P = 0.0192$) were independent risk factors for h-CAM. The cutoff value of AF-IL-8 for predicting each stage of h-CAM (stage I or higher, stage II or higher, and stage III) were ≥9.9 ng/mL, ≥17.3 ng/mL, and ≥55.9 ng/mL, respectively.

Conclusion
The stage of h-CAM was able to be predicted accurately by the level of AF-IL-8 before delivery.

Introduction

Histological chorioamnionitis (h-CAM) is an antenatal inflammatory state of the intrauterine environment strongly associated with preterm delivery. Around 33–83% of infants born before 30–32 weeks of gestation have been exposed to h-CAM,[1–5] which often is a clinically silent process. Exposure to h-CAM is known to induce several organ failures in the fetus.[6] Its presence in placentas from preterm infants increases the incidence of bronchopulmonary dysplasia (BPD),[7–9] necrotizing enterocolitis (NEC),[2,10] periventricular leukomalacia (PVL),[11,12] and cerebral palsy (CP).[12–17] These are recognized as symptoms of fetal response inflammatory syndrome (FIRS).[18–20] These effects have been generally shown to be more pronounced when additional signs of fetal inflammation, such as funisitis, are present.[21–24]

Histological chorioamnionitis is classified into three stages according to Blanc's classification: stage I (deciduitis), stage II (chorionitis), and stage III (amnionitis).[25] van Hoeven et al.[26] reported that the risk of FIRS becomes higher with an increase in the severity of h-CAM. However, the associations between h-CAM and inflammatory markers in maternal circulation have not been fully clarified. On the other hand, clinical CAM was defined by Lenki et al.[27] as maternal fever (≥38.0°C), elevated white blood cell count (≥15,000/μL), uterine tenderness, maternal or fetal tachycardia, and malodorous vaginal fluid. Although clinical CAM may be clearly diagnosed before delivery, neonatal outcomes may already be deteriorated by that point in time,[14,28,29] suggesting that clinical CAM is a final stage of CAM. Park et al.[30] reported that the involvement of the amnion in the inflammatory process of the extraplacental membranes is associated with a more intense fetal inflammatory response than chorionitis alone. Therefore, an accurate prediction of h-CAM and its degree are needed to manage mothers with pre-clinical symptoms of clinical CAM before the appearance of clinical symptoms.

To overcome this problem, the ability of biological markers to detect h-CAM before birth has been investigated. There have been some reports evaluating h-CAM during pregnancy by biological markers, such as maternal body temperature (MBT),[27,31] maternal white blood cell count (WBC),[27,31] maternal C-reactive protein (CRP),[30,32,33] maternal or amniotic interleukin (IL)-6,[34–37] and amniotic IL-8.[38] However, there have been no reports predicting antenatally the severity of h-CAM by biological and clinical markers.

Information about the severity of h-CAM during the antenatal preterm period may be clinically useful for the management of cases at risk for preterm labor or with cervical incompetency. Additionally, with detection of strong intrauterine inflammation before clinical CAM, early termination of the pregnancy may be considered. On the other hand, no detection of inflammation or weak inflammation in the uterus would allow an extended period of pregnancy by maintenance tocolysis. Therefore, the degree of uterine inflammation should be evaluated before delivery, and individual strategies to improve neonatal prognosis for each case should be developed even if there is no sign of clinical CAM.

This study is the first report to show that amniotic fluid IL-8 levels are a good marker for estimating the stage of h-CAM in the antenatal period.

Materials and methods

Study Population

Four hundred and twenty-eight mothers who underwent Cesarean sections were recruited at Toyama University Hospital between January 2009 and December 2013. Two hundred and fifteen cases delivered preterm babies and 213 cases full-term babies. We excluded cases with premature rupture of membranes (PROM), preterm birth within 2 days of maternal steroid treatment leading to increased maternal WBC, severe fetal growth retardation (less than −2.0 S.D.), severe congenital abnormalities, polyhydramnios, gestational diabetes mellitus, preeclampsia, multiple pregnancies, and Cesarean sections due to failure of vaginal trial labor. The study was approved by the ethics committee of Toyama University Hospital. All the subjects included in this study provided informed written consent.

Definitions and Study Procedures

Gestational age was determined from the first day of the last menstrual period, or by fetal size by transvaginal ultrasound before 12 weeks of gestation.

The stages of h-CAM are defined by the degree of the neutrophil infiltration to the amnion–chorion–decidua. The stage I is defined that maternal neutrophils are between the decidua and chorionic plate. The stage II is defined that maternal neutrophils are in the connective tissues of the chorionic plate. Stage III is characterized by neutrophil infiltration of the amnion according to Blanc's diagnostic criteria.[25] And the funisitis was defined as the presence of any vasculitis in the umbilical cord. Section of tissue blocks were stained with hematoxylin–eosin and examined systematically for inflammation by some pathologists unaware of the proteomic results of the amniotic fluid in their laboratory rooms.

Demographic and clinical data (maternal data included age, parity, gestational age at delivery, intrapartum fever, and mode of delivery) were collected. Clinical CAM was defined as the combination of maternal fever during labor (more than 38°C) with any one of the following: maternal tachycardia (≥100 beats/min), uterine tenderness, malodorous amniotic fluid, or maternal leukocytosis (≥15,000 white blood cells/mL).

Poor neonatal outcome was defined as neonatal death or diagnosis of periventricular leukomalacia (PVL), intraventricular hemorrhage (IVH) ≥grade III, bronchopulmonary dysplasia (BPD), and necrotizing enterocolitis (NEC) during hospitalization in the NICU. PVL was defined by de Vries,[39] the classification of IVH was defined by Papile et al.[40] moderate/severe BPD was defined as an oxygen requirement at 36 weeks of gestational age according to the NICHD consensus conference paper,[41] and NEC was defined according to modified Bell's criteria[42] with ≥stage II considered to be significant.

Sample Collection and Preparation

Maternal body temperature was measured just before Cesarean section. In preterm delivery, blood tests (maternal WBC and CRP) were performed within 48 hr before Cesarean section. In the case of elective Cesarean section, which was usually planned at about 39 weeks of gestation in full-term delivery, the blood test was performed within 2 weeks before the Cesarean section. However, in cases with high maternal fever before elective Cesarean section, levels of WBC and CRP were examined again just prior to Cesarean section. Amniotic fluid was extracted directly from the amniotic cavity just before delivery.

Management of Preterm Labor

When the patients are diagnosed as preterm labor, they are immediately hospitalized for bed rest and recommended the treatment of maintenance tocolysis (continuous intravenous infusion of ritodrine hydrochloride or magnesium sulfate) until 36 weeks of gestation to prevent the preterm birth.[43,44] During the long hospitalization, the clinical symptom would go on severer such as bag formation in the cervix, maternal WBC >15,000/μL, or maternal CRP >1.0 mg/dL; intravenous antibiotics (beta-lactam antibiotics 2–3 g/day or EM 800–1500 mg/day for 7 days) are empirically considered by obstetricians. Therefore, we could often use the antibiotics for preterm labor in long hospitalization.

Detection of AF-IL-8

The IL-8 is a chemokine produced by a variety of cell types, and various diseases related as a pro-inflammatory marker were reported.[45–47] We considered that it was a very good marker for the early stage of inflammation in the amnion, and routinely measured amniotic IL-8 level since 2001. In our previous study, amniotic IL-8 level was most reflected at each stage of h-CAM among the level of amniotic IL-8, TNFα, and IL-17.[48]

About 10 mL of amniotic fluid was obtained before delivery. AF-IL-8 was measured by an enzyme-linked immunosorbent assay (ELISA) as previously reported.[49] The detection limit of AF-IL-8 by ELISA was 32 pg/mL. On average, intra-assay and interassay coefficients of variation were 4.8% and 7.5%, respectively. The remaining sample of the amniotic fluid was stored at −80°C.

Statistical Analysis

To identify relevant clinical variables that varied between the h-CAM-positive and h-CAM-negative groups, univariate analysis was performed using the χ^2 test, Student's *t*-test, or Mann–Whitney *U*-test where appropriate. The association between the severity of h-CAM and lower gestational age at delivery was analyzed by ANOVA, and the risk factor of poor neonatal outcome was evaluated by logistic regression analysis. A cutoff value to predict h-CAM was proposed by receiver-operating characteristic (ROC) curves, and logistic regression analysis was performed to investigate the most reliable biochemical marker for the prediction of h-CAM. Odds ratios and 95% confidence intervals (95% CI) were also calculated. Diagnostic values of sensitivity, specificity, positive predictive value (PPV), and negative predictive value (NPV) were estimated to predict h-CAM. The cutoff values to predict the stage of h-CAM were determined using the most reliable biochemical marker. All analyses were performed using statistical analysis software (JMP 9.02; SAS Institute Inc, Tokyo, Japan). A *P* value of below 0.05 was regarded as significant.

Results

The patient characteristics of this study are shown in Table I. There were 215 (50.2%) cases of preterm delivery and 213 (49.8%) cases of full-term delivery. The frequency of stage I, stage II, and stage III h-CAM was 47.4, 35.0, and 17.6%, respectively. Clinical CAM was only detected in h-CAM(+) cases, with the frequency being very low (1.0%). Preterm birth was more frequent, and the gestational age was shorter in h-CAM-positive cases compared to h-CAM-negative cases. Funisitis was observed in 32.5% of h-CAM-positive cases, while it was observed in only 0.8% of h-CAM-negative cases.

There was a significant association between the severity of h-CAM and lower gestational age at delivery (ANOVA; $P < 0.0001$), and the incidence of poor neonatal outcome, such as neonatal death ($n = 4$), PVL ($n = 4$), IVH ≥grade III ($n = 2$), BPD ($n = 11$), and NEC ($n = 1$), was highest (59.1%) in stage III h-CAM (Fig. 1). The severity of h-CAM (odds ratio: 2.7, 95%CI: 1.6–5.0, $P = 0.0004$) and lower gestational age at delivery (odds ratio: 1.3/week, 95%CI: 1.1–1.6, $P = 0.0009$) were independent risk factors of poor neonatal outcome.

Table II shows the averages of four markers (MBT, WBC, CRP, and AF-IL-8) in h-CAM-positive and h-CAM-negative cases. MBT [36.8 (35.1–38.8)°C], WBC [8520 (4500–23,880)/μL], CRP [0.24 (0.02–9.9) mg/dL], and AF-IL-8 [19.7 (0.1–566.5) ng/mL] were significantly higher in h-CAM-positive cases than in h-CAM-negative cases [36.7 (35.0–37.6)°C, 7600 (2490–22,940)/μL, 0.20 (0.02–4.8) mg/dL, and 2.9 (0.1–162.6) ng/mL] ($P < 0.0001$, $P = 0.0002$, $P = 0.0006$, and $P < 0.0001$, respectively). The cutoff values to predict h-CAM were ≥9.9 ng/mL (AF-IL-8), ≥9800/μL (WBC), ≥0.44 mg/dL (CRP), and ≥37.1°C (MBT), respectively (Fig. 2). The area under curve (AUC) of AF-IL-8 (AUC = 0.7653) was significantly larger than those of WBC (AUC = 0.6070), CRP (AUC = 0.5970), and MBT (AUC = 0.6251), respectively ($P < 0.0001$, each) (Fig. 2).

AF-IL-8 (odds ratio: 8.5, 95% CI: 5.1–14.8, $P < 0.0001$) and MBT (odds ratio: 2.3, 95% CI:

Table I Characteristics of Patients ($N = 428$)

	h-CAM (−) ($N = 234$)	h-CAM (+) ($N = 194$)	*P*
Maternal age (year)	33 (18–43)	33 (20–44)	0.3036
Nulliparity (%)	35.9 (84/234)	40.2 (78/194)	0.3602
Antibiotic therapy (%)	6.4 (15/234)	29.9 (58/194)	<0.0001
Preterm birth (%)	41.4 (97/234)	60.8 (118/194)	0.0001
Delivery (w)	37 (24–41)	33 (24–41)	<0.0001
c-CAM (%)	0 (0/234)	1.0 (2/194)	–
Funisitis (%)	0.8 (2/234)	32.5 (63/194)	<0.0001
h-CAM stage I (%)		47.4 (92/194)	–
h-CAM stage II (%)		35.0 (68/194)	–
h-CAM stage III (%)		17.6 (34/194)	–

c-CAM, clinical chorioamnionitis; h-CAM, histological chorioamnionitis.

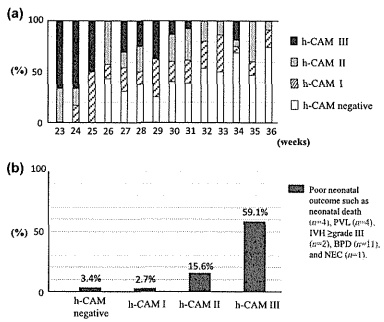

Fig. 1 The ratio of the stage of histological chorioamnionitis (h-CAM) to gestational age at delivery. There was a significant relationship between the severity of h-CAM and lower gestational age at delivery. (ANOVA; $P < 0.0001$) (a) Ratio of poor neonatal prognosis including neonatal death, PVL, IVH ≥stage III, BPD, and NEC. Cases of h-CAM stage III have the highest incidence of poor neonatal prognosis (59.1%) (b).

Table II Clinical Data in Cases With or Without Histological Chorioamnionitis

	h-CAM (−) ($N = 234$)	h-CAM (+) ($N = 194$)	*P*
MBT (°C)	36.7 (35.0–37.6)	36.8 (35.1–38.8)	<0.0001
WBC (/μL)	7600 (2490–22,940)	8520 (4500–23,880)	0.0002
CRP (mg/dL)	0.20 (0.02–4.8)	0.24 (0.02–9.9)	0.0006
AF-IL-8 (ng/mL)	2.9 (0.1–162.6)	19.7 (0.1–566.5)	<0.0001

h-CAM, histological chorioamnionitis; MBT, maternal body temperature; WBC, white blood cell; CRP, C-reactive protein; AF-IL-8, amniotic fluid interleukin-8.

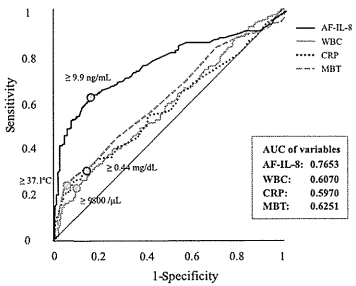

Fig. 2 Receiver-operating curves for amniotic fluid IL-8 (area under curve = 0.7653, $P < 0.0001$ for each AUC of maternal BT, CRP, WBC) for the prediction of histological chorioamnionitis.

1.13–4.1, $P = 0.0192$) were independent risk factors for h-CAM among the four markers (Table III). The level of AF-IL-8 predicted h-CAM with a sensitivity of 57.7%, a specificity of 88.9%, a PPV of 81.1%, and a NPV of 71.7%, while MBT predicted h-CAM with a sensitivity of 27.8%, a specificity of 91.4%, a PPV of 73.0%, and a NPV of 60.4% (Table IV).

Using the level of AF-IL-8, the cutoff value was evaluated to predict the stage of h-CAM before delivery. The cutoff values for h-CAM of stage I or higher, stage II or higher, and stage III were ≥9.9, ≥17.3, and ≥ 55.9 ng/mL, respectively (Fig. 3). The sensitivities for predicting h-CAM of stage I or higher, stage II or higher, and stage III were 57.7, 77.4, and 91.2%, with specificities of 88.9, 85.3, and 91.4%, respectively (Table V).

Although the frequency of funisitis was significantly increased with increase in the stage of h-CAM (Table VI), AF-IL-8 levels in each stage of h-CAM with or without funisitis were similar (Table VII).

Table III Logistic Regression Analysis for the Prediction of Histological Chorioamnionitis

	Odds ratio	95% CI	*P*
MBT (>37.1°C)	2.3	1.13–4.1	0.0192
WBC (>9800/μL)	1.1	0.62–1.9	0.7204
CRP (>0.44 mg/dL)	1.3	0.77–2.3	0.2986
AF-IL-8 (>9.9 ng/mL)	8.5	5.1–14.8	<0.0001

CI, confidence interval; MBT, maternal body temperature; WBC, white blood cell; CRP, C-reactive protein; AF-IL-8, amniotic fluid interleukin-8.

Discussion

Strengths and Weakness of the Study

The following are major strengths of this study. (i) This study was comprised of a large cohort of women with singleton babies ($N = 428$) and with histologic chorioamnionitis ($N = 194$). (ii) We evaluated several markers of infection and inflammation including AF-IL-8, MBT, WBC, and CRP. We found both AF-IL-8 and MBT were independent markers to predict h-CAM before delivery, and the predictive value for h-CAM was higher in AF-IL-8 compared to MBT. (iii) We have shown for the first time that the level of AF-IL-8 was able to estimate the stage of h-CAM before delivery. The cutoff value of AF-IL-8 to predict stage I or higher was ≥9.9 ng/mL with a sensitivity of 57.7% and a specificity of 88.9%. The cutoff value to predict stage II or higher was ≥17.3 ng/mL with a sensitivity of 77.4% and a specificity of 85.3%. The cutoff value to predict stage III of h-CAM was ≥55.9 ng/mL with a sensitivity of 91.2% and a specificity of 91.4%. (iv) In our study, poor neonatal prognosis, such as neonatal death, PVL, IVH ≥grade III, BPD, and NEC, was extremely high in cases of stage III h-CAM. When h-CAM stage III is estimated by AF-IL-8 level, termination of pregnancy may be considered. However, the gestational age at that point in time must also be considered for fetal prematurity.

Table IV Diagnostic Factors for the Prediction of Histological Chorioamnionitis

	Sensitivity (%)	Specificity (%)	PPV (%)	NPV (%)
AF-IL-8 (>9.9 ng/mL)	57.7 (112/194)	88.9 (208/234)	81.1 (112/138)	71.7 (208/290)
MBT (>37.1°C)	27.8 (54/194)	91.4 (214/234)	73.0 (54/74)	60.4 (214/354)

AF-IL-8, amniotic fluid interleukin-8; MBT, maternal body temperature; PPV, positive predictive value; NPV, negative predictive value.

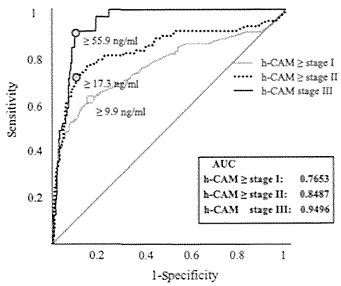

Fig. 3 Cutoff values of amniotic fluid IL-8 to predict the stages of histological chorioamnionitis. The area under curve for the prediction of histological chorioamnionitis stage I or higher, stage II or higher, and stage III is 0.7653, 0.8487, and 0.9496, respectively.

The following are potential weaknesses of this study. (i) While in most cases WBC and CRP were examined just prior to Cesarean section, some full-term delivery cases without symptoms were examined within 2 weeks. (ii) We report no information about the levels of other cytokines in the amniotic fluid. Amniotic IL-8 level was measured because it has been reported that amniotic fluid IL-8 levels gradually increased with the h-CAM stage.[48] Amniotic TNF-α and IL-17 levels are only elevated in stage III of h-CAM.[48] Holst et al.[50] reported that among 27 proteins in the amnion, amniotic macrophage protein-1β (MIP-1β) is useful to predict delivery within 7 days. Keeler et al.[51] also reported that among 25 amniotic cytokines, monocyte chemotactic protein-1 (MCP-1) is the best marker for the prediction of early delivery. Using these suggested amniotic markers reflecting strong inflammation in the amnion, further detail of h-CAM may be able to be provided. Further studies are needed to clarify which cytokines are the best suited to evaluate the stage of h-CAM. (iii) When the stage III of h-CAM will be predicted by amniotic IL-8 levels, certainly, the best treatment was not leaded in this study. However, using this result of predicting the accurate stage of h-CAM antenatally, the new strategy might be effective to prevent the neonatal outcomes in the future studies.

Table VI Frequency of Funisitis in Each Stage of Histological Chorioamnionitis

h-CAM	Frequency of funisitis		
Stage I	8.7 (8/92)	$P < 0.0001$	$P < 0.0001$
Stage II	43.9 (29/68)	$P = 0.0012$	
Stage III	76.5 (26/34)		

h-CAM, histological chorioamnionitis.

Table VII Association between Amniotic Fluid IL-8 and Funisitis in Each Stage of Histological Chorioamnionitis

	Funisitis (+)	Funisitis (–)	*P*
AF-IL-8 (ng/mL)			
Stage I	12.5 (0.1–40.2)	5.8 (0.1–240.6)	0.4142
Stage II	21.2 (0.1–379.5)	39.6 (0.1–376.7)	0.6944
Stage III	165.6 (17.5–566.5)	118.7 (26.5–237.5)	0.1679

h-CAM, histological chorioamnionitis; AF-IL-8, amniotic fluid interleukin-8.

Clinical Significance of this Study

Lenki et al.[27] reported that clinical CAM may be diagnosed by symptoms and blood examination, although the prognosis of the neonate is usually poor by the time clinical CAM is made evident.[10,28] This study reported a very low frequency of clinical CAM, suggesting that the majority of the h-CAM cases were terminated before the onset of clinical CAM. This evidence prompted us to establish a new

Table V Diagnostic Factors for the Prediction of Histological Chorioamnionitis Stages

	Sensitivity (%)	Specificity (%)	PPV (%)	NPV (%)
h-CAM > stage I (>9.9 ng/mL)	57.7 (112/194)	88.9 (208/234)	81.1 (112/138)	71.7 (208/290)
h-CAM > stage II (>17.3 ng/mL)	77.4 (79/102)	85.3 (278/326)	62.2 (79/127)	92.3 (278/301)
h-CAM stage III (>55.9 ng/mL)	91.2 (31/34)	91.4 (360/394)	47.7 (31/65)	99.2 (360/363)

h-CAM, histological chorioamnionitis; PPV, positive predictive value; NPV, negative predictive value.

strategy for diagnosing h-CAM before the appearance of clinical signs. Therefore, recognition of h-CAM as a pre-stage of clinical chorioamnionitis may allow better management of women at risk for preterm labor or cervical incompetency and avoid poor neonatal prognosis such as neonatal death, PVL, IVH ≥grade III, BPD, and NEC.

An accurate prediction of the stage of h-CAM is important to provide proper treatment. Compared to cases with h-CAM, pregnancies without h-CAM should be extended as long as possible. Although there has been no evidence showing the efficacy of maintenance tocolysis for treatment, it may be effective for treatment of low-grade h-CAM predicted antenatally. Knowing the estimated grade of h-CAM, we may be able to determine an appropriate time for delivery in cases of severe intrauterine inflammation to avoid a poor outcome for the baby. We have reported that clinical symptoms and AF-IL-8 may be used to estimate the time of delivery in preterm labor cases.[52]

The aim of this study was only to lead the cutoff value of amniotic IL-8 levels to predict each stage of h-CAM by using large number of amniotic samples. Therefore, the sample included cases of the third trimester. The evaluation of amniocentesis to predict the stage of h-CAM was clinically for less than 30 weeks of gestation.

The Correlation between AF-IL-8 and Funisitis

It was reported that the risk of FIRS increases with the presence of h-CAM. The severity of h-CAM influences FIRS, although the degree of influence on the fetus is unknown. Funisitis can also increase the risk of FIRS.[21–24] In the present study, there was no correlation between the level of AF-IL-8 and funisitis in any of the stages of h-CAM (Table VI). The level of AF-IL-8 was strongly correlated with the stage of h-CAM, irrespective of the existence of funisitis. These data suggested that AF-IL-8 is a good marker for h-CAM, but not for predicting funisitis.

Questions in this Study

The antibiotic therapy has the effect just to microbes, not inflammation. And the preterm delivery was strongly correlated with amniotic inflammation (h-CAM) rather than the microbes in the amnion.[53,54] Therefore, antibiotic therapy was considered not to influence the amniotic fluid IL-8 levels.

Despite the high rate of preterm birth of 41% in h-CAM-negative group, the rate of delivery before 33 weeks of gestation was 14.9% (35/234) without h-CAM, while 38.6% (75/194) with h-CAM. The rate of preterm delivery of 41% was certainly high; however, most cases were delivered after 33 weeks of gestation without h-CAM.

The frequency of clinical CAM was only 1%: The reason was considered that (i) in this study, we excluded the premature rupture of the membranes (PROM) that often happened to clinical CAM. (ii) A large numbers of sample cases after 33 weeks of gestations were included in our study (73.8%).

Unanswered Questions and Proposals for Future Research

At present, the stage of h-CAM cannot predict the condition of the baby before delivery. Therefore, a prediction of the stage of h-CAM as part of the management of cases at risk for preterm labor or cervical incompetency may improve the prognosis of neonates. Maintenance tocolysis may be performed in cases without h-CAM or with h-CAM stage I, while a short-term tocolysis may be carried out in cases with h-CAM stage II or III. In cases with h-CAM stage III and with a positive microbubble test showing fetal lung maturation, delivery of the baby should be considered as an option, taking into account the gestational age. In conclusion, the stage of h-CAM may be predicted accurately by the level of AF-IL-8 before delivery.

References

1 Lahra MM, Jeffery HE: A fetal response to chorioamnionitis is associated with early survival after preterm birth. *Am J Obstet Gynecol* 2004; 190:147–151.

2 Been JV, Rours IG, Kornelisse RF, Lima Passos V, Kramer BW, Schneider TA, de Krijger RR, Zimmermann LJ: Histologic chorioamnionitis, fetal involvement, and antenatal steroids: effects on neonatal outcome in preterm infants. *Am J Obstet Gynecol* 2009; 201:587. e581–588.

3 Been JV, Zimmermann LJ: Histological chorioamnionitis and respiratory outcome in preterm infants. *Arch Dis Child Fetal Neonatal Ed* 2009; 94:F218–F225.

4 Erdemir G, Kultursay N, Calkavur S, Zekioğlu O, Koroglu OA, Cakmak B, Yalaz M, Akisu M, Sagol S: Histological chorioamnionitis: effects on premature delivery and neonatal prognosis. *Pediatr Neonatol* 2013; 54:267–274.

5 Ogunyemi D, Murillo M, Jackson U, Hunter N, Alperson B: The relationship between placental histopathology findings and perinatal outcome in preterm infants. *J Matern Fetal Neonatal Med* 2003; 13:102–109.

6 Gantert M, Been JV, Gavilanes AW, Garnier Y, Zimmermann LJ, Kramer BW: Chorioamnionitis: a multiorgan disease of the fetus? *J Perinatol* 2010; 30:S21–S30.

7 Kotecha S: Cytokines in chronic lung disease of prematurity. *Eur J Pediatr* 1996; 155:S14–S17.

8 Speer CP: Inflammatory mechanisms in neonatal chronic lung disease. *Eur J Pediatr* 1999; 158:S18–S22.

9 Zanardo V, Vedovato S, Trevisanuto DD, Suppiej A, Cosmi E, Fais GF, Chiarelli S: Histological chorioamnionitis and neonatal leukemoid reaction in low-birth-weight infants. *Hum Pathol* 2006; 37:87–91.

10 Been JV, Lievense S, Zimmermann LJ, Kramer BW, Wolfs TG: Chorioamnionitis as a Risk Factor for Necrotizing Enterocolitis: a Systematic Review and Meta-Analysis. *J Pediatr* 2013; 162:236–242. e2.

11 Yoon BH, Romero R, Yang SH, Jun JK, Kim IO, Choi JH, Syn HC: Interleukin-6 concentrations in umbilical cord plasma are elevated in neonates with white matter lesions associated with periventricular leukomalacia. *Am J Obstet Gynecol* 1996; 174:1433–1440.

12 Wu YW, Colford JM Jr: Chorioamnionitis as a risk factor for cerebral palsy: a meta-analysis. *JAMA* 2000; 284:1417–1424.

13 Bashiri A, Burstein E, Mazor M: Cerebral palsy and fetal inflammatory response syndrome: a review. *J Perinat Med* 2006; 34:5–12.

14 Yoon BH, Park CW, Chaiworapongsa T: Intrauterine infection and the development of cerebral palsy. *BJOG* 2003; 110:124–127.

15 Yoon BH, Romero R, Park JS, Kim CJ, Kim SH, Choi JH, Han TR: Fetal exposure to an intra-amniotic inflammation and the development of cerebral palsy at the age of three years. *Am J Obstet Gynecol* 2000; 182:675–681.

16 Soraisham AS, Trevenen C, Wood S, Singhal N, Sauve R: Histological chorioamnionitis and neurodevelopmental outcome in preterm infants. *J Perinatol* 2013; 33:70–75.

17 Shatrov JG, Birch SC, Lam LT, Quinlivan JA, McIntyre S, Mendz GL: Chorioamnionitis and cerebral palsy: a meta-analysis. *Obstet Gynecol* 2010; 116:387–392.

18 Hofer N, Kothari R, Morris N, Müller W, Resch B: The fetal inflammatory response syndrome is a risk factor for morbidity in preterm neonates. *Am J Obstet Gynecol* 2013; 209:542. e1-542.e11.

19 Gomez R, Romero R, Ghezzi F, Yoon BH, Mazor M, Berry SM: The fetal inflammatory response syndrome. *Am J Obstet Gynecol* 1998; 179:194–202.

20 Gotsch F, Romero R, Kusanovic JP, Mazaki-Tovi S, Pineles BL, Erez O, Espinoza J, Hassan SS: The fetal inflammatory response syndrome. *Clin Obstet Gynecol* 2007; 50:652–683.

21 Lahra MM, Beeby PJ, Jeffery HE: Maternal versus fetal inflammation and respiratory distress syndrome: a 10-year hospital cohort study. *Arch Dis Child Fetal Neonatal Ed* 2009; 94:F13–F16.

22 D'Alquen D, Kramer BW, Seidenspinner S, Marx A, Berg D, Groneck P, Speer CP: Activation of umbilical cord endothelial cells and fetal inflammatory response in preterm infants with chorioamnionitis and funisitis. *Pediatr Res* 2005; 57:263–269.

23 Pacora P, Chaiworapongsa T, Maymon E, Kim YM, Gomez R, Yoon BH, Ghezzi F, Berry SM, Qureshi F, Jacques SM, Kim JC, Kadar N, Romero R: Funisitis and chorionic vasculitis: the histological counterpart of the fetal inflammatory response syndrome. *J Matern Fetal Neonatal Med* 2002; 11:18–25.

24 Kim CJ, Yoon BH, Park SS, Kim MH, Chi JG: Acute funisitis of preterm but not term placentas is associated with severe fetal inflammatory response. *Hum Pathol* 2001; 32:623–629.

25 Blanc WA: Pathology of the placenta, membranes and umbilical cord in bacterial, fungal, and viral infections in man. *In* Perinatal Disease, RL Naeye (ed). Baltimore, Williams & Wilkins, 1981, pp 67–132.

26 van Hoeven KH, Anyaegbunam A, Hochster H, Whitty JE, Distant J, Crawford C, Factor SM: Clinical significance of increasing histologic severity of acute inflammation in the fetal membranes and umbilical cord. *Pediat Pathol Lab Med* 1996; 16:731–744.

27 Lenki SG, Maciulla MB, Eglinton GS: Maternal and umbilical cord serum interleukin level in preterm labor with clinical chorioamnionitis. *Am J Obstet Gynecol* 1994; 170:1345–1351.

28 Lieberman E, Lang J, Richardson DK, Frigoletto FD, Heffner LJ, Cohen A: Intrapartum maternal fever and neonatal outcome. *Pediatrics* 2000; 105:8–13.

29 Nasef N, Shabaan AE, Schurr P, Iaboni D, Choudhury J, Church P, Dunn MS: Effect of clinical and histological chorioamnionitis on the outcome of preterm infants. *Am J Perinatol* 2013; 30:59–68.

30 Park CW, Moon KC, Park JS, Jun JK, Romero R, Yoon BH: The involvement of human amnion in histologic chorioamnionitis is an indicator that a fetal and an intra-amniotic inflammatory response is more likely and severe: clinical implications. *Placenta* 2009; 30:56–61.

31 Roberts DJ, Celi AC, Riley LE, Onderdonk AB, Boyd TK, Johnson LC, Lieberman E: Acute histologic chorioamnionitis at term: nearly always noninfectious. *PLoS ONE* 2012; 7:e31819.

32 van de Laar R, van der Ham DP, Oei SG, Willekes C, Weiner CP, Mol BW: Accuracy of C-reactive protein determination in predicting chorioamnionitis and neonatal infection in pregnant women with premature rupture of membranes: a systematic review. *Eur J Obstet Gynecol Reprod Biol* 2009; 147:124–129.

33 Trochez-Martinez RD, Smith P, Lamont RF: Use of C-reactive protein as a predictor of chorioamnionitis in preterm prelabour rupture of membranes: a systematic review. *BJOG* 2007; 114:796–801.

34 Maeda K, Matsuzaki N, Fuke S, Mitsuda N, Shimoya K, Nakayama M, Suehara N, Aono T: Value of the maternal interleukin 6 level for determination of histologic chorioamnionitis in preterm delivery. *Gynecol Obstet Invest* 1997; 43:225–231.

35 Gulati S, Bhatnagar S, Raghunandan C, Bhattacharjee J: Interleukin-6 as a predictor of subclinical chorioamnionitis in preterm premature rupture of membranes. *Am J Reprod Immunol* 2012; 67:235–240.

36 Kacerovsky M, Musilova I, Hornychova H, Kutova R, Pliskova L, Kostal M, Jacobsson B: Bedside assessment of amniotic fluid interleukin-6 in preterm prelabor rupture of membranes. *Am J Obstet Gynecol* 2014; 211:385. e1-9.

37 Cobo T, Kacerovsky M, Palacio M, Hornychova H, Hougaard DM, Skogstrand K, Jacobsson B: A prediction model of histological chorioamnionitis and funisitis in preterm prelabor rupture of membranes: analyses of multiple proteins in the amniotic fluid. *J Matern Fetal Neonatal Med* 2012; 25:1995–2001.

38 Kacerovsky M, Drahosova M, Hornychova H, Pliskova L, Bolehovska R, Forstl M, Tosner J, Andrys C: Value of amniotic fluid interleukin-8 for the prediction of histological chorioamnionitis in preterm premature rupture of membranes. *Neuro Endocrinol Lett* 2009; 30:733–738.

39 de Vries LS, Eken P, Dubowitz LM: The spectrum of leukomalacia using cranial ultrasound. *Behav Brain Res* 1992; 49:1–6.

40 Papile LA, Burstein J, Burstein R, Koffler H: Incidence and evolution of subependymal and intraventricular hemorrhage: a study of infants with birth weights less than 1,500 gm. *J Pediatr* 1978; 92:529–534.

41 Jobe AH, Bancalari E: Bronchopulmonary dysplasia. *Am J Respir Crit Care Med* 2001; 163:1723–1729.

42 Walsh MC, Kliegman RM: Necrotizing enterocolitis: treatment based on staging criteria. *Pediatr Clin North Am* 1986; 33:179–201.

43 Plummer CP: Evaluation of maternal and neonatal outcomes after maintenance tocolysis: a retrospective study. *J Obstet Gynaecol Res* 2012; 38:198–202.

44 Yaju Y, Nakayama T: Effectiveness and safety of ritodrine hydrochloride for the treatment of preterm labour: a systematic review. *Pharmacoepidemiol Drug Saf* 2006; 15:813–822.

45 Guerrini A, Mancini I, Maietti S, Rossi D, Poli F, Sacchetti G, Gambari R, Borgatti M: Expression of pro-inflammatory interleukin-8 is reduced by ayurvedic decoctions. *Phytother Res* 2014; 28:1173–1181.

46 Quan J, Liu J, Gao X, Liu J, Yang H, Chen W, Li W, Li Y, Yang W, Wang B: Palmitate induces interleukin-8 expression in human aortic vascular smooth muscle cells via Toll-like receptor 4/nuclear factor-κB pathway (TLR4/NF-κB-8). *J Diabetes* 2014; 6:33–41.

47 Cielecka-Kuszyk J, Siennicka J, Jabłońska J, Rek O, Godzik P, Rabczenko D, Madaliński K: Is interleukin-8 an additional to histopathological changes diagnostic marker in HCV-infected patients with cryoglobulinemia? *Hepatol Int* 2011; 5:934–940.

48 Ito M, Nakashima A, Hidaka T, Okabe M, Bac ND, Ina S, Yoneda S, Shiozaki A, Sumi S, Tsuneyama K, Nikaido T, Saito S: A role for IL-17 in induction of an inflammation at the fetomaternal interface in preterm labour. *J Reprod Immunol* 2010; 84:75–85.

49 Luo L, Ibaragi T, Maeda M, Nozawa M, Kasahara T, Sakai M, Sasaki Y, Tanebe K, Saito S: Interleukin-8 levels and granulocyte counts in cervical mucus during pregnancy. *Am J Reprod Immunol* 2000; 43:78–84.

50 Holst RM, Hagberg H, Wennerholm UB, Skogstrand K, Thorsen P, Jacobsson B: Prediction of spontaneous preterm delivery in women with preterm labor: analysis of multiple proteins in amniotic and cervical fluids. *Obstet Gynecol* 2009; 114: 268–277.

51 Keeler SM, Kiefer DG, Rust OA, Vintzileos A, Atlas RO, Bornstein E, Hanna N: Comprehensive amniotic fluid cytokine profile evaluation in women with a short cervix: which cytokine(s) correlates best with outcome? *Am J Obstet Gynecol* 2009; 201:276. e1-6.

52 Yoneda S, Shiozaki A, Yoneda N, Shima T, Ito M, Yamanaka M, Hidaka T, Sumi S, Saito S: Prediction of exact delivery time in patients with preterm labor and intact membranes at admission by amniotic fluid interleukin-8 level and preterm labor index. *J Obstet Gynaecol Res* 2011; 37:861–866.

53 Coultrip LL, Lien JM, Gomez R, Kapernick P, Khoury A, Grossman JH: The value of amniotic fluid interleukin-6 determination in patients with preterm labor and intact membranes in the detection of microbial invasion of the amniotic cavity. *Am J Obstet Gynecol* 1994; 171:901–911.

54 Romero R, Yoon BH, Mazor M, Gomez R, Diamond MP, Kenney JS, Ramirez M, Fidel PL, Sorokin Y, Cotton D: The diagnostic and prognostic value of amniotic fluid white blood cell count, glucose, interleukin-6, and gram stain in patients with preterm labor and intact membranes. *Am J Obstet Gynecol* 1993; 169: 805–816.

Contents lists available at ScienceDirect

Journal of Reproductive Immunology

journal homepage: www.elsevier.com/locate/jreprimm

Helios-positive functional regulatory T cells are decreased in decidua of miscarriage cases with normal fetal chromosomal content

Kumiko Inada, Tomoko Shima, Mika Ito, Akemi Ushijima, Shigeru Saito*

Department of Obstetrics and Gynecology, University of Toyama, Toyama 930-0194, Japan

ARTICLE INFO

Article history:
Received 10 June 2014
Received in revised form 9 September 2014
Accepted 10 September 2014

Keywords:
Effector Treg
Helios
Human pregnancy
Miscarriage
Naturally occurring Treg

ABSTRACT

Regulatory (Treg) T cells play essential roles in the maintenance of allogeneic pregnancy in mice and humans. Recent data show that Foxp3 expression occurs in both immunosuppressive Treg and -nonsuppressive effector T (Teff) cells upon activation in humans. Samstein et al. (2012) reported that inducible Treg (iTreg) cells enforce maternal–fetal tolerance in placental mammals. Therefore, we should reanalyze which types of Treg cell play an important role in the maintenance of allogeneic pregnancy. In this study, we studied the frequencies of naïve Treg cells, effector Treg cells, Foxp3$^+$ Teff cells, Helios$^+$ naturally occurring Treg (nTreg) cells, and Helios$^-$ iTreg cells using flow cytometry. The frequencies of effector Treg cells and Foxp3$^+$ Teff cells among CD4$^+$Foxp3$^+$ cells in the decidua of miscarriage cases with a normal embryo karyotype ($n=8$) were significantly lower ($P=0.0105$) and significantly higher ($P=0.0258$) than those in normally progressing pregnancies ($n=11$), respectively. However, these frequencies in miscarriages with an abnormal embryo karyotype ($n=15$) were similar to those in normally progressing pregnancies. The frequencies of these cell populations in the three groups were unchanged in peripheral blood; on the other hand, most of the effector Treg cells in the decidua were Helios$^+$ nTreg cells and these frequencies were significantly higher than those in peripheral blood, while those among effector Treg and naïve Treg cells in the decidua and peripheral blood were similar among the three groups. These data suggest that decreased Helios$^+$ effector nTreg might play an important role in the maintenance of pregnancy in humans.

1. Introduction

Regulatory T cells (Treg) play an important role in the induction and maintenance of tolerance (Sakaguchi et al., 1995; Sakaguchi, 2005). In 2004, Aluvihare et al. and our group first reported that Treg cells might mediate maternal tolerance to the fetus in mice and humans (Aluvihare et al., 2004; Sasaki et al., 2004). Since then, many lines of evidence supporting the importance of Treg cells in the implantation period and the early pregnancy period have been presented, with more detailed characterization of Treg cells in mice (Zenclussen et al., 2005, 2006; Darrasse-Jèze et al., 2006; Kallikourdis et al., 2007; Robertson et al., 2009; Shima et al., 2010; Kahn and Baltimore, 2010; Guerin et al., 2011; Rowe et al., 2011, 2012; Samstein et al., 2012; Yin et al., 2012) and in humans (Tilburgs et al., 2008, 2009; Sasaki et al., 2007; Yang et al., 2008; Jin et al., 2009; Mei et al., 2010; Wang et al., 2010, 2011; Winger and Reed, 2011; Lee et al., 2011; Steinborn et al., 2012).

For example, adoptive transfer of Treg cells purified from normal pregnant mice prevented fetal loss in CBA/Jφ × DBA/2J ♂ mice (Zenclussen et al., 2005; Yin et al., 2012), suggesting that fetal antigen-specific Treg cells might play essential roles in the maintenance of allogeneic pregnancy. Seminal plasma plays an important role in the expansion of fetal antigen-specific Treg (Robertson et al., 2009; Guerin et al., 2011). Memory Treg cells that recognize paternal antigens also rapidly increase in a second pregnancy with the same partner compared with the first (Rowe et al., 2012). A decreased Treg cell pool was observed in recurrent miscarriage cases in humans (Yang et al., 2008; Jin et al., 2009; Mei et al., 2010; Wang et al., 2010, 2011; Lee et al., 2011) and a low Treg cell level predicts the risk of miscarriage in cases of unexplained recurrent pregnancy loss (Winger and Reed, 2011). Selective migration of fetus-specific Treg cells from the peripheral blood to the decidua in human pregnancy has also been reported (Tilburgs et al., 2008). We have reported that the population of CD4$^+$Foxp3$^+$ Treg cells at the decidua basalis in miscarriage with a normal karyotype embryo was significantly lower than in normally progressing pregnancy and in miscarriage with an abnormal embryo, suggesting that dysregulation of maternal tolerance to the fetus might be associated with unknown etiology of miscarriage in humans (Inada et al., 2013).

We considered that Foxp3 is the most reliable marker for Treg cells (Hori et al., 2003), but recent data have shown that Foxp3$^+$ expression in humans occurs in both immunosuppressive Treg cells and non-suppressive and cytokine-producing effector T cells (Walker et al., 2003; Gavin et al., 2006; Allan et al., 2007). Miyara et al. (2009) reported that human CD4$^+$Foxp3$^+$ cells are classified into CD4$^+$CD45RA$^+$Foxp3^{low} naïve Treg cells, CD4$^+$CD45RA$^-$Foxp3^{high} effector Treg cells, and CD4$^+$CD45RA$^-$Foxp3^{low} effector T (Teff) cells. Importantly, those Foxp3$^+$ Teff cells have no capacity for immunoregulation. CD4$^+$CD25^{bright} T cells exhibit regulatory function in humans (Beacher-Allan et al., 2001). Miyara et al. (2009) showed that CD4$^+$CD25^{bright} cells are composed of CD4$^+$CD45RA$^+$Foxp3^{low} naïve T cells, CD4$^+$CD45RA$^-$Foxp3^{low} Teff cells, and CD4$^+$CD45RA$^-$Foxp3^{high} effector Treg cells. CD4$^+$CD25$^+$CD127$^-$ cells are believed to be a reliable marker for Treg cells (Seddiki et al., 2006), but Kleinewietfeld et al. (2009) pointed out that some of the CD4$^+$CD25$^+$CD127$^-$ cells are Teff cells, which produce IFN-γ, IL-2, and IL-17. These findings suggest that we should re-evaluate which subsets of Foxp3$^+$ cells play an important role in the maintenance of pregnancy.

Treg cells are classified as naturally occurring Treg (nTreg) generated in the thymus and inducible T (iTreg) generated in the periphery (Sakaguchi, 2005). Samstein et al. (2012) reported that conserved noncoding sequence 1 (CNS1), which is essential for iTreg differentiation, is conserved only in placental mammals, and CNS1-deficient female mice showed increased fetal resorption in allogeneic pregnancy. These findings suggest that iTreg induction at the fetomaternal interface might be important for a successful pregnancy in placental mammals.

However, it has still not been reported which subset of Treg cells is important for the maintenance of human pregnancy: naive Treg cells, effector Treg cells, nTregs or iTregs. As such, we have studied the populations of naïve Treg cells, effector Treg cells, Foxp3$^+$ Teff cells, Helios$^+$ nTreg cells, and Helios$^-$ iTreg cells in the decidua or peripheral blood of miscarriage cases with abnormal or normal fetal chromosomal content.

2. Materials and methods

2.1. Cases of normal pregnancy and miscarriage

This study was approved by the Ethics Committee of the University of Toyama. We obtained written informed consent from all the cases. We enrolled 11 subjects with normally progressing pregnancy, 15 with miscarriage and an abnormal embryo karyotype (trisomy [$n=14$] including trisomy8 [$n=2$], trisomy13 [$n=2$], trisomy15 [$n=1$], trisomy16 [$n=3$], trisomy21 [$n=3$], trisomy22 [$n=3$], and translocation [$n=1$]), and 8 with miscarriage and a normal embryo karyotype. Chorionic villi were sampled from miscarriage cells for cytogenetic analysis. Fetal chromosomal karyotyping was performed by conventional G-band staining. Echo sonography was performed every two weeks, and patients were advised to obtain an induced abortion if the fetal heartbeat ceased or was never detected. In women with a normally progressing pregnancy, fetal heartbeat was identified before elective termination. None of the subjects had any risk factors such as genetic abnormalities (neither themselves nor their husband), uterine malformation, thyroid dysfunction or anti-phospholipid antibody syndrome.

The clinical background in these groups is shown in Table 1. The numbers of previous miscarriages in women miscarrying with an abnormal embryo and miscarrying with a normal embryo were significantly higher than in the normal pregnancy group. Gestational weeks at sampling, body mass index (BMI), and frequency of smoking were similar among the three groups.

2.2. Flow cytometry

Decidual mononuclear cells (leukocytes) were purified by the Ficoll Hypaque method after homogenization and filtration through a 32-μm nylon mesh, as previously reported (Saito et al., 1992).

The following monoclonal antibodies (mAbs) were used in this study: anti-CD4 (Per CP-Cy5.5; BD Biosciences, NJ, USA), anti-CD45RA (Biotin; BD Bioscience), and streptavidin labeled with APC-Cy7 (BD Biosciences) as cell surface markers, and anti-Foxp3 (FITC; eBioscience, San Diego, CA, USA) and anti-Helios (Alexa Fluor 647; eBioscience) as intracellular markers. Decidual and peripheral mononuclear cells were first stained with anti-CD4 mAb and anti-CD45RA mAb for 30 min on ice. Cells were washed with phosphate-buffered saline (PBS) three times. Next, APC-Cy7-labeled streptavidin was added and inoculated for 15 min on ice. After washing the cells with PBS three times, they were fixed and permeabilized by incubation for 30 min with fixation/permeabilization buffer (eBioscience), and then stained with anti-Foxp3 and anti-Helios mAb. Flow cytometry analysis was performed on a BD FACScanII (BD Biosciences).

Lymphocytes were gated based on both forward and side scatter parameters (Fig. 1, left). Monocytes,

* Corresponding author. Tel.: +81 76 434 7355; fax: +81 76 434 5036.
E-mail address: s30saito@med.u-toyama.ac.jp (S. Saito).

http://dx.doi.org/10.1016/j.jri.2014.09.053
0165-0378/

Table 1
Clinical background in normal pregnancy, miscarriage with an abnormal embryo and miscarriage with a normal embryo.

	Normal pregnancy $n=11$	Miscarriage with an abnormal embryo $n=15$	Miscarriage with a normal embryo $n=8$
Age (year)*	27.5 ± 0.7 (16–39)	37.3 ± 0.3 (29–44)†	32.1 ± 0.8 (22–42)
Gravidities*,**	1.0 ± 0.1 (0–2)	2.2 ± 0.08 (0–4)†	2.5 ± 0.2 (0–5)
Nulliparity	6/11 (54.5%)	10/15 (66.7%)	4/8 (50.0%)
No. of liveborn children*	0.7 ± 0.08 (0–2)	0.3 ± 0.03 (0–1)	0.5 ± 0.07 (0–1)
No. of miscarriages*,***	0 (0–0)	2.5 ± 0.08 (1–5)††	2.8 ± 0.2 (1–5)††
Stillbirth*	0 (0–0)	0.1 ± 0.02 (0–1)	0 (0–0)
Gestational weeks*	7.5 ± 0.2 (6–10)	7.2 ± 0.09 (5–10)	6.1 ± 0.2 (5–9)
BMI*	20.4 ± 0.2 (17.7–23.1)	21.8 ± 0.2 (17.7–27.1)	20.6 ± 0.4 (18.0–27.7)
Smoker	3/11 (27.2%)	1/15 (6.7%)	0/8 (0%)

* Mean ± SEM (range).
** This pregnancy or miscarriage is not included in gravidities.
*** This miscarriage is included in no. of miscarriages.
† $P<0.05$ vs. normal pregnancy.
†† $P<0.001$ vs. normal pregnancy.
††† $P<0.0001$ vs. normal pregnancy.

granulocytes, and decidual stromal cells were excluded from the setting of a lymphocyte gate as in Fig. 1 (left). After gating on $CD4^+$ cells (Fig. 1, center), the proportions of $CD4^+CD45RA^+Foxp3^{low}$ naïve Treg, $CD4^+CD45RA^-Foxp3^{high}$ effector Treg, and $CD4^+CD45RA^-Foxp3^{low}$ Teff cells were determined among $CD4^+Foxp3^+$ cells (Fig. 1). Isotype-matched fluorochrome-conjugated mice IgG were used as a control. $Foxp3^{low}$ and $Foxp3^{high}$ were classified as follows. In the peripheral blood, some of the $CD4^+$ cells expressed $Foxp3^{low}$ (Fig. 1, upper column). The expression of Foxp3 in $Foxp3^{high}$ cells was brighter than those in $CD4^+Foxp3^{low}$ cells. In the decidua, $CD4^+Foxp3^{high}$ cells formed a cluster, and we classified these as $CD4^+Foxp3^{high}$ cells and $CD4^+Foxp3^{low}$ cells (Fig. 1, center and right).

2.3. Statistical analysis

Statistical analysis was performed using a statistical software package (SAS version 9.1; SAS Institute, USA). Data were analyzed using the Mann–Whitney U test. A value of $P<0.05$ was considered statistically significant.

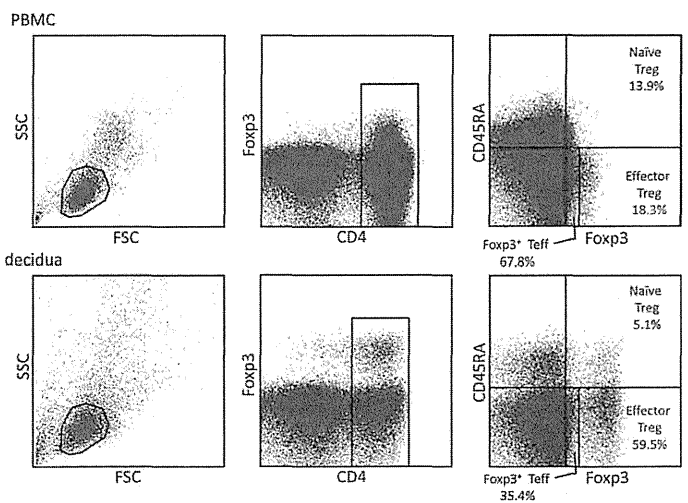

Fig. 1. Gating strategy for the detection of $CD4^+CD45RA^+Foxp3^{low}$ naïve Treg cells, $CD4^+45RA^-Foxp3^{high}$ effector Treg cells, and $CD4^+CD45RA^-Foxp3^{low}$ effector T cells. Lymphocytes in the peripheral blood (upper column) and decidua (lower column) were gated on forward and side scatter parameters. $CD4^+$ T cells in peripheral blood and decidua were classified into $CD45RA^+Foxp3^{low}$ cells, $CD45RA^-Foxp3^{high}$ effector Treg cells, and $CD45RA^-Foxp3^{low}$ Teff cells. The percentages of $CD45RA^+Foxp3^{low}$ cells, $CD45RA^-Foxp3^{high}$ cells, and $CD45RA^-Foxp3^{low}$ cells among $CD4^+Foxp3^+$ T cells are displayed.

3. Results

3.1. Frequencies of $Foxp3^+$ cells and Treg (naïve Treg + effector Treg) cells among $CD4^+$ cells in the decidua

The frequency of decidual $Foxp3^+$ cells among $CD4^+$ cells in miscarriage cases with normal fetal chromosomal content was significantly lower ($P=0.039$) than that in normal pregnancies (Fig. 2A). However, this frequency in miscarriage cases with abnormal chromosomal content was similar to that in normal pregnancies. Next, we measured the frequency of Treg cells (naïve Treg cells + effector Treg cells) among $CD4^+$ T cells. The frequency of the true Treg cell population excluding $Foxp3^+$ Teff cells in the decidua was significantly lower in subjects with miscarriage and a normal embryo karyotype than in those with normal pregnancies, and in subjects with miscarriage and an abnormal embryo karyotype ($P=0.0258$ and $P=0.0389$ respectively; Fig. 2B). We have reanalyzed the frequency of decidual $Foxp3^+$ cells and true Treg cells in subjects with a first pregnancy (○), subjects who have had a previous live birth (●), and the subjects with miscarriage who have had previous miscarriage(s) and no live births (△). There were no significant differences in $Foxp3^+$ cells and true Treg cells among the three groups, although the sample size is small.

3.2. Frequencies of decidual naïve Treg cells, effector Treg cells and $Foxp3^+$ Teff cells among $CD4^+Foxp3^+$ cells

The frequency of decidual effector Treg cells in subjects with miscarriage and a normal embryo karyotype was significantly lower ($P=0.0105$) than that in subjects with normal pregnancies (Fig. 3B). On the other hand, the frequency of decidual $Foxp3^+$ Teff cells in subjects with miscarriage and a normal embryo karyotype was significantly higher than that in subjects with normal pregnancies and in subjects with miscarriage and an abnormal embryo ($P=0.0258$ and $P=0.0389$ respectively; Fig. 3C). The ratio of effector Treg cells to $Foxp3^+$ Teff cells in subjects with miscarriage and a normal embryo was significantly lower ($P=0.0106$) than that in subjects with normal pregnancies.

The frequencies of naïve Treg cells were similar among the three groups (Fig. 3A).

3.3. Frequency of naïve Treg cells, effector Treg cells and $Foxp3^+$ Teff cells among $CD4^+Foxp3^+$ cells in the peripheral blood

The frequencies of naïve Treg cells, effector Treg cells and $Foxp3^+$ Teff cells in the peripheral blood were similar among the three groups (Fig. 4A–C). The frequency of effector Treg cells in the peripheral blood in subjects with miscarriage and a normal karyotype embryo appeared to be higher, but the difference did not reach significance (Fig. 4B). $Foxp3^+$ Teff cell population in peripheral blood did not increase in subjects with miscarriage and a normal karyotype embryo. Furthermore, the ratio of effector Treg cells to $Foxp3^+$ Teff cells in subjects with miscarriage and a normal embryo karyotype appeared to be higher, but the difference did not reach significance (Fig. 4D). The frequency of effector Treg cells and $Foxp3^+$ Teff cells was different between decidua and peripheral blood. We have calculated the ratio of the frequency of decidual naïve Treg cells to that of peripheral Treg cells (Fig. 5A), frequency of

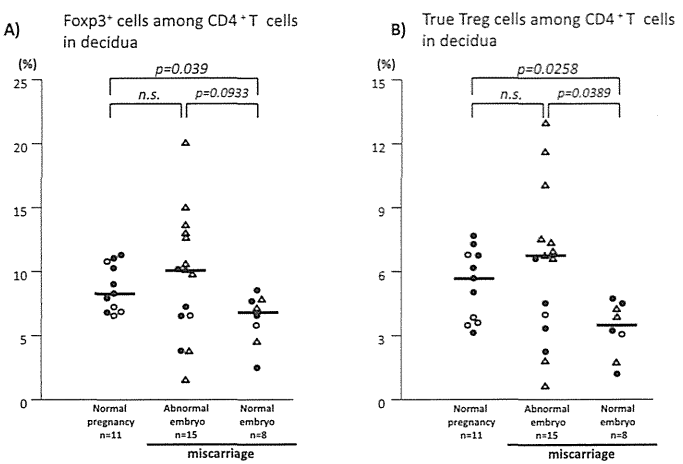

Fig. 2. Frequencies of $Foxp3^+$ cells (A) and true Treg (naïve Treg and effector Treg) cells (B) among $CD4^+$ cells in the decidua of normal pregnancy, miscarriage with abnormal karyotype embryo and miscarriage with normal karyotype embryo. Horizontal bar is the median value. n.s. means not significant. Open circle shows subjects with their first pregnancy. Closed circle shows subjects who have had a previous live birth. Open triangle shows the subjects with miscarriage who have had a previous miscarriage(s) and no live births.

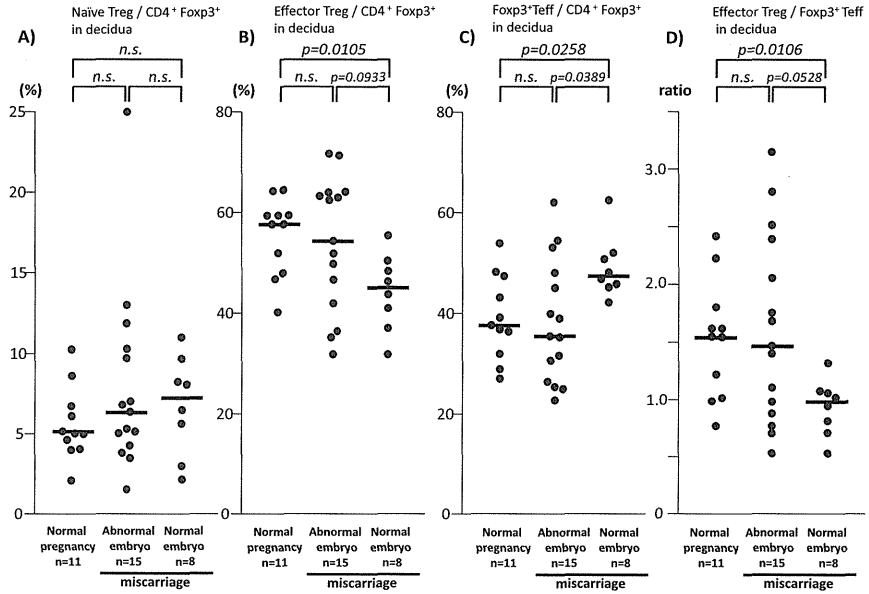

Fig. 3. Frequencies of decidual naïve Treg cells (A), effector Treg cells (B), and Foxp3+ Teff cells (C) among CD4+Foxp3+ cells, and the ratio of effector Treg cells/Foxp3+ Teff cells (D) in normal pregnancy, miscarriage with abnormal karyotype embryo, and miscarriage with normal karyotype embryo. Horizontal bar is the median value. n.s. means not significant.

decidual effector Treg cells to that of the peripheral blood (Fig. 5B), and frequency of decidual Foxp3+ Teff cells to that of the peripheral blood (Fig. 5C). The ratio of effector Treg cells of decidua to peripheral blood in subjects with miscarriage and a normal karyotype embryo was significantly lower than that in subjects with normal pregnancies and in subjects with miscarriage and an abnormal karyotype embryo ($P=0.0128$ and $P=0.0123$ respectively; Fig. 5B). The ratio of Foxp3+ Teff cells of the decidua to those in the peripheral blood was significantly higher ($P=0.0265$) in subjects with miscarriage and a normal karyotype embryo than the ratio in subjects with normal pregnancies, and in subjects with miscarriage and an abnormal karyotype embryo ($P=0.0265$ and $P=0.0066$ respectively; Fig. 5C).

3.4. Frequency of Helios+ effector Treg cells and naïve Treg cells in the decidua and peripheral blood of normal pregnancies, miscarriages with an abnormal karyotype embryo, and miscarriages with a normal karyotype embryo

The frequency of Helios+ Treg cells in the peripheral blood was around 80% of normal pregnancies, miscarriages with an abnormal karyotype embryo, and in miscarriages with a normal karyotype embryo, as previously reported (Thornton et al., 2010; Fig. 6A). The frequencies of Helios+ naïve Treg cells were similar between decidua and peripheral blood in normal pregnancies, miscarriages with abnormal karyotype embryo, and miscarriages with normal karyotype embryo (Fig. 6A). However, the frequency of Helios+ effector Treg cells in the decidua was over 90%, and this frequency in the decidua was significantly higher than in peripheral blood in normal pregnancies ($P=0.02$), miscarriages with abnormal karyotype embryo ($P=0.008$), and miscarriages with a normal karyotype embryo ($P=0.02$) in contrast to the data for naïve Treg cells (Fig. 6B), suggesting the selective migration of effector Treg cells into the decidua from peripheral blood. However, the frequencies of Helios+ cells among effector Treg cells in the decidua and peripheral blood were similar among the three groups. On the other hand, the frequencies of Helios+-naïve Treg cells were similar to those in decidua and peripheral blood (Fig. 6A).

Next, we studied the frequency of Helios-positive or Helios-negative naïve Treg cells and effector Treg cells in the decidua (Table 2). The frequency of decidual Helios+ effector Treg cells among CD4+Foxp3+cells in subjects with miscarriage and a normal embryo was significantly lower compared with that in normal pregnancy subjects ($P=0.0258$). These frequencies in the peripheral blood were similar among the three groups (Table 3).

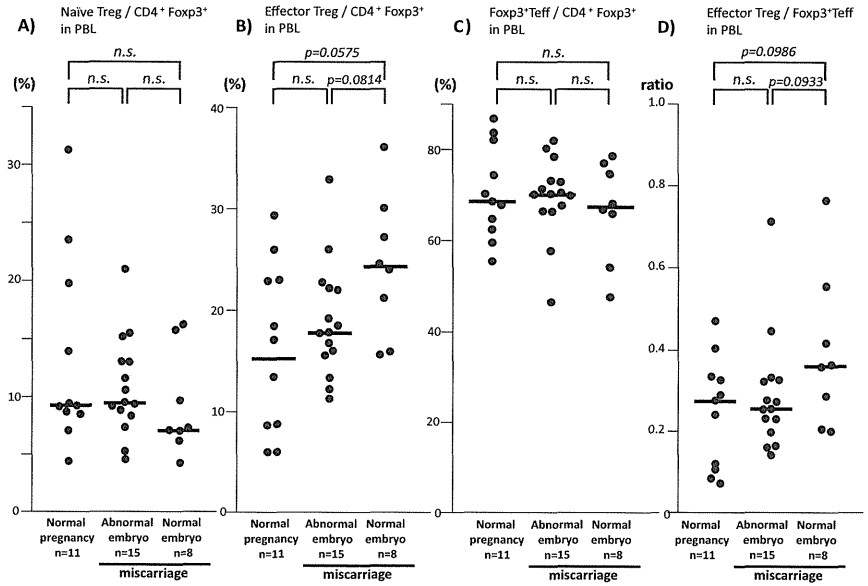

Fig. 4. Frequencies of peripheral blood naïve Treg cells (A), effector Treg cells (B), and Foxp3+ Teff cells (C) among CD4+Foxp3+ cells, and the ratio of effector Treg cells/Foxp3+ Teff cells (D) in normal pregnancy, miscarriage with abnormal karyotype embryo, and miscarriage with normal karyotype embryo. Horizontal bar shows the median value. n.s. means not significant.

Table 2
Frequencies of decidual Helios-positive or Helios-negative naïve Treg cells and effector Treg cells in normal pregnancy, miscarriage with an abnormal embryo and miscarriage with a normal embryo.

	Normal pregnancy $n=11$	Miscarriage with an abnormal embryo $n=15$	Miscarriage with a normal embryo $n=8$
Helios+ naïve Treg cells/CD4+Foxp3+ cells (%)*	4.03 ± 0.20 (0.81–9.08)	6.77 ± 0.37 (1.22–24.07)	5.48 ± 0.35 (1.12–8.53)
Helios− naïve Treg cells/CD4+Foxp3+ cells (%)*	1.53 ± 0.18 (0.49–7.33)	1.13 ± 0.054 (0.23–3.15)	1.14 ± 0.088 (0.54–2.44)
Helios+ effector Treg cells/CD4+Foxp3+ cells (%)*	52.99 ± 0.78 (37.84–64.03)	51.69 ± 0.90 (30.16–71.29)	42.83 ± 0.98 (30.11–54.54)†
Helios− effector Treg cells/CD4+Foxp3+ cells (%)*	2.30 ± 0.17 (0.58–6.81)	2.12 ± 0.18 (0.26–8.74)	1.42 ± 0.12 (0.31–3.47)

* Mean ± SEM (range).
† $P<0.05$ vs. normal pregnancy.

Table 3
Frequencies of peripheral blood Helios-positive or Helios-negative naïve Treg cells and effector Treg cells in normal pregnancy, miscarriage with an abnormal embryo and miscarriage with a normal embryo.

	Normal pregnancy $n=11$	Miscarriage with an abnormal embryo $n=15$	Miscarriage with a normal embryo $n=8$
Helios+ naïve Treg cells/CD4+Foxp3+ cells (%)*	10.41 ± 0.96 (4.77–23.10)	8.09 ± 0.21 (3.09–14.60)	6.74 ± 0.39 (4.10–12.01)
Helios− naïve Treg cells/CD4+Foxp3+ cells (%)*	4.21 ± 0.40 (1.55–8.25)	2.53 ± 0.15 (0–6.8)	2.49 ± 0.19 (0–5.27)
Helios+ effector Treg cells/CD4+Foxp3+ cells (%)*	7.25 ± 0.37 (4.14–11.11)	7.41 ± 0.34 (2.40–20.8)	5.78 ± 0.41 (1.91–10.30)
Helios− effector Treg cells/CD4+Foxp3+ cells (%)*	1.28 ± 0.13 (0.53–2.80)	1.76 ± 0.093 (0–5.08)	0.83 ± 0.099 (0–2.11)

* Mean ± SEM (range).

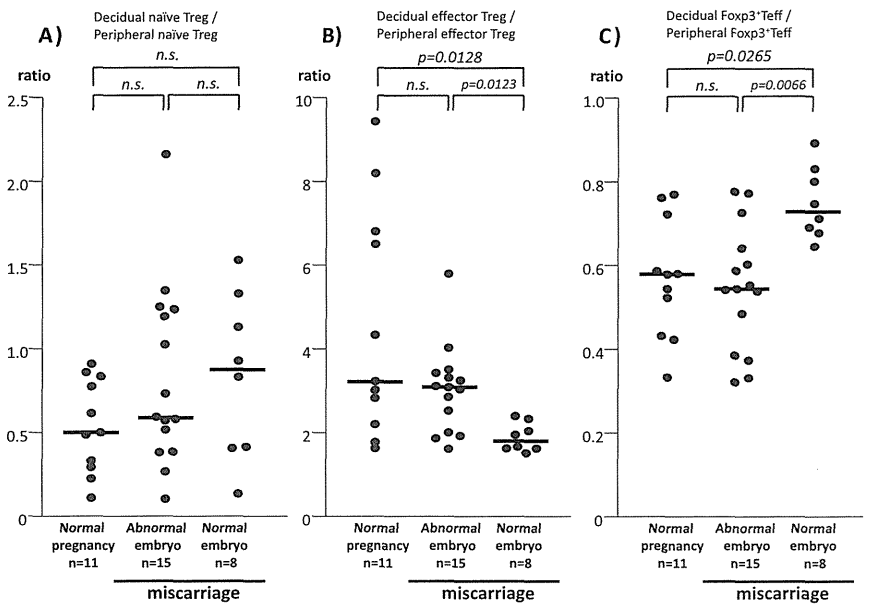

Fig. 5. The ratio of naïve Treg cells in decidua to those in peripheral blood (A), the ratio of effector Treg cells in decidua to those in peripheral blood (B), and the ratio of Foxp3⁺ Teff cells in decidua to those in peripheral blood (C). Horizontal bar shows the medium value. n.s. means not significant.

4. Discussion

Foxp3 is believed to be a specific marker for Treg cells (Hori et al., 2003), but recent data show that Foxp3 expression transiently occurs in IL-2- and IFN-γ-producing Teff cells in humans (Walker et al., 2003; Gavin et al., 2006; Allan et al., 2007). It is possible that these activated Teff cells might react to fetal antigens presented by antigen-presenting cells (APCs) in the decidua and create harmful inflammation causing demise of the embryo. Many papers have reported that Foxp3⁺ cells increase in normal pregnancy, but decrease in miscarriage (Sasaki et al., 2004; Yang et al., 2008; Jin et al., 2009; Mei et al., 2010; Wang et al., 2010, 2011; Lee et al., 2011) and preeclampsia (Sasaki et al., 2007; Santner-Nanan et al., 2009). However, there are no reports describing which types of Foxp3⁺ cell increase or decrease in miscarriage. Foxp3⁺ cells are classified into effector Treg cells that contribute to immune tolerance, naïve Treg cells that show a weak capacity for immunoregulation, and Teff cells that break immune tolerance. This is the first report that shows that decidual effector Treg cells decreased in miscarriage with a normal karyotype embryo, but not in miscarriage with an abnormal karyotype embryo. Interestingly, Foxp3⁺ Teff cells in the decidua were increased in miscarriage with a normal karyotype embryo. The immunological environment is controlled by the balance between immunoactivation and immunoregulation. In the miscarriage cases with a normal karyotype embryo, the balance seemed to shift to an immunoactivation-dominant state, and dysregulation of tolerance to the fetus might occur. We compared the percentage of effector Treg cells and Foxp3⁺ Teff in CD4⁺Foxp3 cells in decidua and peripheral blood. Our findings suggest that immunological abnormality might be limited in the pregnant uterus in miscarriage with a normal karyotype embryo. Unfortunately, we did not measure the weight of decidual samples; therefore, we could not calculate the numbers of these cells in milligrams of decidua. This is a limitation of our study.

The etiology of recurrent pregnancy loss (RPL) is unknown in 40–60% of cases (Clifford et al., 1994). In a murine model, decreased Treg cells could induce implantation failure (Darrasse-Jèze et al., 2006; Shima et al., 2010) and early pregnancy loss by activation of T cells and NK cells (Aluvihare et al., 2004; Zenclussen et al., 2005; Thaxton et al., 2013), suggesting that immune dysregulation might be one of the etiologies of fetal resorption. These findings suggest that a proportion of sporadic miscarriage cases or RPL cases with a normal fetal karyotype might be associated with the immune etiology of miscarriage in humans. However, further studies are needed to prove this.

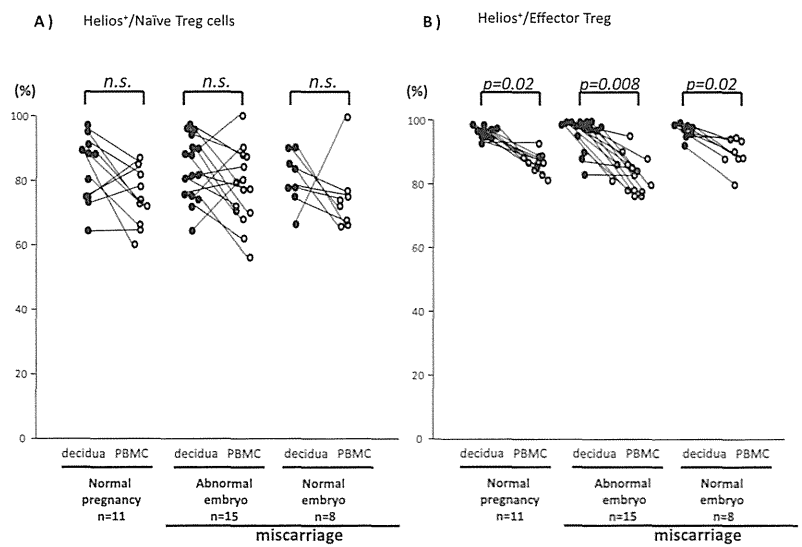

Fig. 6. Helios-positive naïve Treg cells (A) and effector Treg cells (B) in the decidua and peripheral blood of subjects with normal pregnancy, subjects with miscarriage and an abnormal karyotype embryo, and subjects with miscarriage and a normal karyotype embryo. PBMC, peripheral blood mononuclear cells.

Samstein et al. (2012) recently reported that a Foxp3 enhancer, CNS1, is essential for the induction of iTreg cells and that iTreg cells play an essential role in the maintenance of allogeneic pregnancy in placental animals. Thornton et al. (2010) reported that Helios, an Ikaros transcription factor family member, is a specific marker of nTreg cells. Therefore, we analyzed Helios⁺ nTreg cells and Helios⁻ iTreg cells among effector Treg cells in the decidua and peripheral blood. Our data first showed that there were very few Helios⁻ iTreg cells in the decidua of subjects with normal pregnancy and also in that of human subjects with miscarriage, and that the frequency of Helios⁻ iTreg did not change in miscarriage. Furthermore, the frequency of Helios⁺ functional nTreg in the decidua was significantly higher than that in peripheral blood in normal pregnancies, miscarriages with an abnormal karyotype embryo and miscarriage with a normal karyotype embryo, but the frequency of Helios⁺ naïve nTreg cells in the decidua was similar to that in peripheral blood. This finding may be explained by the fact that Helios⁺ functional nTreg cells selectively accumulated in the pregnant uterus from the periphery. Indeed, selective migration of fetus-specific Treg cells from the peripheral blood to the decidua was reported in human pregnancy (Tilburgs et al., 2008) and murine pregnancy (Kallikourdis et al., 2007). We have already reported that there were decreased numbers of Foxp3⁺ cells at the decidua basalis were decreased, but not at the decidua parietalis, in subjects with miscarriage and a normal embryo karyotype, showing the failure of the migration of Treg cells at the fetomaternal interface (Inada et al., 2013). The level of effector Treg cells in peripheral blood was slightly elevated in subjects with miscarriages and a normal karyotype embryo (Fig. 4B), which may indirectly support this idea. Indeed, Chen et al. (2013) recently showed that $CD44^{high}$ $CD62L^{low}$ activated memory Treg cells specific for self-antigen were rapidly recruited to the uterus-draining lymph nodes and activated in the first days after embryo implantation. Further studies are necessary to discover whether self-specific memory Treg cells are nTreg or iTreg cells. In summary, Helios⁺ effector Treg cells were decreased in the decidua of subjects with miscarriage and a normal karyotype embryo. Effector nTreg may play an important role in the maintenance of pregnancy in humans, although Helios is not a strict marker for nTreg (Zabransky et al., 2012).

It is well known that the Treg cell pool is decreased in preeclampsia (Sasaki et al., 2007; Santner-Nanan et al., 2009) and recent data showed that Helios⁻ iTreg cells, but not Helios⁺ nTreg cells, were decreased in peripheral blood in preeclampsia (Hsu et al., 2012). iTreg cells may be important for the maintenance of pregnancy at a late stage. Indeed, Rowe et al. (2012) reported that the frequency of Helios⁺ fetal antigen-specific nTreg cells in mid-gestation (11.5 days post-coitus) was 70%, and this frequency in late gestation (18.5 days post-coitus) was reduced to 40%, suggesting that Helios⁻ fetal antigen specific iTreg cells expanded in late pregnancy. Neuropilin 1 is expressed on nTreg cells (Weiss et al., 2012; Yadav et al., 2012). We have

tried to study the expression of neuropilin 1 on Treg cells, but the immunostaining of neuropilin 1 was weak; thus, we could not classify Treg cells into nTreg and iTreg cells using neuropilin 1 staining.

Rowe et al. (2012) reported that memory Treg cells that sustain anergy to fetal antigen play a role in the rapid induction of fetomaternal tolerance. Importantly, when Treg cells from female mice were transferred into pregnant mice soon after delivery, they quickly expanded after pregnancy, but when Foxp3$^-$CD4$^+$ T cells were transferred into pregnant mice, donor-derived fetal antigen-specific Treg cells did not appear (Rowe et al., 2012). If iTreg cells play an essential role in the maintenance of allogeneic pregnancy, donor-derived fetal antigen-specific iTreg cells should be increased, but Helios$^+$-fetal antigen-specific nTreg cells were the major population in mid-gestation (Rowe et al., 2012). Furthermore, when CNS1-deficient female mice were mated with allogeneic male mice, the resorption rate was only 10% (Samstein et al., 2012). More than 50% resorption was observed when total Treg cells were depleted in mice (Shima et al., 2010; Rowe et al., 2012). This finding suggests that not only iTreg cells, but also nTreg cells, might play a role in a successful pregnancy. Further studies are needed on the types of Treg cell that play an important role in successful implantation and pregnancy in mice and humans.

In conclusion, we are, to our knowledge, the first to show that Helios-positive functional Treg cells decreased and Foxp3$^+$ Teff cells increased in the decidua of miscarriage cases with normal fetal chromosomal content. These findings suggest that dysregulation of fetomaternal tolerance might be one of the etiologies of miscarriage in humans.

Disclosure

None of the authors has any conflict of interest related to this manuscript.

Acknowledgements

This work was supported by grants from the Ministry of Education, Culture, Sports, Science, and Technology of Japan [a Grant-in-Aid for Scientific Research (B) 23390386, a Grant-in-Aid for Young Scientists (B) 23791818, and a Grant-in-Aid for Young Scientists (B) 24791107].

References

Allan, S.E., Crome, S.Q., Crellin, N.K., Passerini, L., Steiner, T.S., Bacchetta, R., Roncarolo, M.G., Levings, M.K., 2007. Activation-induced FOXP3 in human T effector cells does not suppress proliferation or cytokine production. Int. Immunol. 19, 345–354.

Aluvihare, V.R., Kallikourdis, M., Betz, A.G., 2004. Regulatory T cells mediate maternal tolerance to the fetus. Nat. Immunol. 5, 266–271.

Beacher-Allan, C., Brown, J.A., Freeman, G.J., Hafler, D.A., 2001. CD4+CD25high regulatory cells in human peripheral blood. J. Immunol. 167, 1245–1253.

Chen, T., Darrasse-Jèze, G., Bergot, A.S., Courau, T., Churlaud, G., Valdivia, K., Strominger, J.L., Ruocco, M.G., Chaouat, G., Klatzmann, D., 2013. Self-specific memory regulatory T cells protect embryos at implantation in mice. J. Immunol. 191, 2273–2281.

Clifford, K., Rai, R., Watson, H., Regan, L., 1994. An informative protocol for the investigation of recurrent miscarriage: preliminary experience of 500 consecutive cases. Hum. Reprod. 9, 1328–1332.

Darrasse-Jèze, G., Klatzmann, D., Charlotte, F., Salomon, B.L., Cohen, J.L., 2006. CD4+CD25+ regulatory/suppressor T cells prevent allogeneic fetus rejection in mice. Immunol. Lett. 102, 106–109.

Gavin, M.A., Torgerson, T.R., Houston, E., DeRoos, P., Ho, W.Y., Stray-Pedersen, A., Ocheltree, E.L., Greenberg, P.D., Ochs, H.D., Rudensky, A.Y., 2006. Single-cell analysis of normal and FOXP3-mutant human T cells: FOXP3 expression without regulatory T cell development. Proc. Natl. Acad. Sci. U.S.A. 103, 6659–6664.

Guerin, L.R., Moldenhauer, L.M., Prins, J.R., Bromfield, J.J., Hayball, J.D., Robertson, S.A., 2011. Seminal fluid regulates accumulation of FOXP3+ regulatory T cells in the preimplantation mouse uterus through expanding the FOXP3+ cell pool and CCL19-mediated recruitment. Biol. Reprod. 85, 397–408.

Hori, S., Nomura, T., Sakaguchi, S., 2003. Control of regulatory T cell development by the transcription factor Foxp3. Science 299, 1057–1061.

Hsu, P., Santner-Nanan, B., Dahlstrom, J.E., Fadia, M., Chandra, A., Peek, M., Nanan, R., 2012. Altered decidual DC-SIGN+ antigen-presenting cells and impaired regulatory T-cell induction in preeclampsia. Am. J. Pathol. 181, 2149–2160.

Inada, K., Shima, T., Nakashima, A., Aoki, K., Ito, M., Saito, S., 2013. Characterization of regulatory T cells in decidua of miscarriage cases with abnormal or normal fetal chromosomal content. J. Reprod. Immunol. 97, 104–111.

Jin, L.P., Chen, Q.Y., Zhang, T., Guo, P.F., Li, D.J., 2009. The CD4+CD25 bright regulatory T cells and CTLA-4 expression in peripheral and decidual lymphocytes are down-regulated in human miscarriage. Clin. Immunol. 133, 402–410.

Kahn, D.A., Baltimore, D., 2010. Pregnancy induces a fetal antigen-specific maternal T regulatory cell response that contributes to tolerance. Proc. Natl. Acad. Sci. U.S.A. 107, 9299–9304.

Kallikourdis, M., Andersen, K.G., Welch, K.A., Betz, A.G., 2007. Alloantigen-enhanced accumulation of CCR5+ 'effector' regulatory T cells in the gravid uterus. Proc. Natl. Acad. Sci. U.S.A. 104, 594–599.

Kleinewietfeld, M., Starke, M., Di Mitri, D., Borsellino, G., Battistini, L., Rötzschke, O., Falk, K., 2009. CD49d provides access to untouched human Foxp3+ Treg free of contaminating effector cells. Blood 113, 827–836.

Lee, S.K., Kim, J.Y., Hur, S.E., Kim, C.J., Na, B.J., Lee, M., Gilman-Sachs, A., Kwak-Kim, J., 2011. An imbalance in interleukin-17-producing T and Foxp3+ regulatory T cells in women with idiopathic recurrent pregnancy loss. Hum. Reprod. 26, 2964–2971.

Mei, S., Tan, J., Chen, H., Chen, Y., Zhang, J., 2010. Changes of CD4+CD25high regulatory T cells and FOXP3 expression in unexplained recurrent spontaneous abortion patients. Fertil. Steril. 94, 2244–2247.

Miyara, M., Yoshioka, Y., Kitoh, A., Shima, T., Wing, K., Niwa, A., Parizot, C., Taflin, C., Heike, T., Valeyre, D., Mathian, A., Nakahata, T., Yamaguchi, T., Nomura, T., Ono, M., Amoura, Z., Gorochov, G., Sakaguchi, S., 2009. Functional delineation and differentiation dynamics of human CD4+ T cells expressing the FoxP3 transcription factor. Immunity 30, 899–911.

Robertson, S.A., Guerin, L.R., Bromfield, J.J., Branson, K.M., Ahlström, A.C., Care, A.S., 2009. Seminal fluid drives expansion of the CD4+CD25+ T regulatory cell pool and induces tolerance to paternal alloantigens in mice. Biol. Reprod. 80, 1036–1045.

Rowe, J.H., Ertelt, J.M., Aguilera, M.N., Farrar, M.A., Way, S.S., 2011. Foxp3(+) regulatory T cell expansion required for sustaining pregnancy compromises host defense against prenatal bacterial pathogens. Cell Host Microbe 10, 54–64.

Rowe, J.H., Ertelt, J.M., Xin, L., Way, S.S., 2012. Pregnancy imprints regulatory memory that sustains anergy to fetal antigen. Nature 490, 102–106.

Saito, S., Nishikawa, K., Morii, T., Narita, N., Enomoto, M., Ichijo, M., 1992. Expression of activation antigens CD69, HLA-DR, interleukin-2 receptor-alpha (IL-2R alpha) and IL-2R beta on T cells of human decidua at an early stage of pregnancy. Immunol. 75, 710–712.

Sakaguchi, S., Sakaguchi, N., Asano, M., Itoh, M., Toda, M., 1995. Immunologic self-tolerance maintained by activated T cells expressing IL-2 receptor alpha-chains (CD25). Breakdown of a single mechanism of self-tolerance causes various autoimmune diseases. J. Immunol. 155, 1151–1164.

Sakaguchi, S., 2005. Naturally arising Foxp3-expressing CD25+CD4+ regulatory T cells in immunological tolerance to self and non-self. Nat. Immunol. 6, 345–352.

Samstein, R.M., Josefowicz, S.Z., Arvey, A., Treuting, P.M., Rudensky, A.Y., 2012. Extrathymic generation of regulatory T cells in placental mammals mitigates maternal–fetal conflict. Cell 150, 29–38.

Santner-Nanan, B., Peek, M.J., Khanam, R., Richarts, L., Zhu, E., Fazekas de St Groth, B., Nanan, R., 2009. Systemic increase in the ratio between Foxp3+ and IL-17-producing CD4+ T cells in healthy pregnancy but not in preeclampsia. J. Immunol. 183, 7023–7030.

Sasaki, Y., Sakai, M., Miyazaki, S., Higuma, S., Shiozaki, A., Saito, S., 2004. Decidual and peripheral blood CD4+CD25+ regulatory T cells in early pregnancy subjects and spontaneous abortion cases. Mol. Hum. Reprod. 10, 347–353.

Sasaki, Y., Darmochwal-Kolarz, D., Suzuki, D., Sakai, M., Ito, M., Shima, T., Shiozaki, A., Rolinski, J., Saito, S., 2007. Proportion of peripheral blood and decidual CD4(+) CD25(bright) regulatory T cells in pre-eclampsia. Clin. Exp. Immunol. 149, 139–145.

Seddiki, N., Santner-Nanan, B., Martinson, J., Zaunders, J., Sasson, S., Landay, A., Solomon, M., Selby, W., Alexander, S.I., Nanan, R., Kelleher, A., Fazekas de St Groth, B., 2006. Expression of interleukin (IL)-2 and IL-7 receptors discriminates between human regulatory and activated T cells. J. Exp. Med. 203, 1693–1700.

Shima, T., Sasaki, Y., Itoh, M., Nakashima, A., Ishii, N., Sugamura, K., Saito, S., 2010. Regulatory T cells are necessary for implantation and maintenance of early pregnancy but not late pregnancy in allogeneic mice. J. Reprod. Immunol. 85, 121–129.

Steinborn, A., Schmitt, E., Kisielewicz, A., Rechenberg, S., Seissler, N., Mahnke, K., Schaier, M., Zeier, M., Sohn, C., 2012. Pregnancy-associated diseases are characterized by the composition of the systemic regulatory T cell (Treg) pool with distinct subsets of Tregs. Clin. Exp. Immunol. 167, 84–98.

Thaxton, J.E., Nevers, T., Lippe, E.O., Blois, S.M., Saito, S., Sharma, S., 2013. NKG2D blockade inhibits poly(I:C)-triggered fetal loss in wild type but not in IL-1 0-/- mice. J. Immunol. 190, 3639–3647.

Thornton, A.M., Korty, P.E., Tran, D.Q., Wohlfert, E.A., Murray, P.E., Belkaid, Y., Shevach, E.M., 2010. Expression of Helios, an Ikaros transcription factor family member, differentiates thymic-derived from peripherally induced Foxp3+ T regulatory cells. J. Immunol. 184, 3433–3441.

Tilburgs, T., Roelen, D.L., van der Mast, B.J., de Groot-Swings, G.M., Kleijburg, C., Scherjon, S.A., Claas, F.H., 2008. Evidence for a selective migration of fetus-specific CD4+CD25bright regulatory T cells from the peripheral blood to the decidua in human pregnancy. J. Immunol. 180, 5737–5745.

Tilburgs, T., Scherjon, S.A., van der Mast, B.J., Haasnoot, G.W., Versteeg, V.D., Voort-Maarschalk, M., Roelen, D.L., van Rood, J.J., Claas, F.H., 2009. Fetal–maternal HLA-C mismatch is associated with decidual T cell activation and induction of functional T regulatory cells. J. Reprod. Immunol. 82, 148–157.

Walker, M.R., Kasprowicz, D.J., Gersuk, V.H., Benard, A., Van Landeghen, M., Buckner, J.H., Ziegler, S.F., 2003. Induction of FoxP3 and acquisition of T regulatory activity by stimulated human CD4+CD25– T cells. J. Clin. Invest. 112, 1437–1443.

Wang, W.J., Hao, C.F., Q. u., Q.L., Wang, X., Qiu, L.H., Lin, Q.D., 2010. The deregulation of regulatory T cells on interleukin-17-producing T helper cells in patients with unexplained early recurrent miscarriage. Hum. Reprod. 25, 2591–2596.

Wang, W.J., Hao, C.F., Lin, Q.D., 2011. Dysregulation of macrophage activation by decidual regulatory T cells in unexplained recurrent miscarriage patients. J. Reprod. Immunol. 92, 97–102.

Weiss, J.M., Bilate, A.M., Gobert, M., Ding, Y., Curotto de Lafaille, M.A., Parkhurst, C.N., Xiong, H., Dolpady, J., Frey, A.B., Ruocco, M.G., Yang, Y., Floess, S., Huehn, J., Oh, S., Li, M.O., Niec, R.E., Rudensky, A.Y., Dustin, M.L., Littman, D.R., Lafaille, J.J., 2012. Neuropilin 1 is expressed on thymus-derived natural regulatory T cells, but not mucosa-generated induced Foxp3+ T reg cells. J. Exp. Med. 209, 1723–1742.

Winger, E.E., Reed, J.L., 2011. Low circulating CD4(+) CD25(+) Foxp3(+) T regulatory cell levels predict miscarriage risk in newly pregnant women with a history of failure. Am. J. Reprod. Immunol. 66, 320–328.

Yadav, M., Louvet, C., Davini, D., Gardner, J.M., Martinez-Llordella, M., Bailey-Bucktrout, S., Anthony, B.A., Sverdrup, F.M., Head, R., Kuster, D.J., Ruminski, P., Weiss, D., Von Schack, D., Bluestone, J.A., 2012. Neuropilin-1 distinguishes natural and inducible regulatory T cells among regulatory T cell subsets in vivo. J. Exp. Med. 209, 1713–1722.

Yang, H., Qiu, L., Chen, G., Ye, Z., Lü, C., Lin, Q., 2008. Proportional change of CD4+CD25+ regulatory T cells in decidua and peripheral blood in unexplained recurrent spontaneous abortion patients. Fertil. Steril. 89, 656–661.

Yin, Y., Han, X., Shi, Q., Zhao, Y., He, Y., 2012. Adoptive transfer of CD4+CD25+ regulatory T cells for prevention and treatment of spontaneous abortion. Eur. J. Obstet. Gynecol. Reprod. Biol. 161, 177–181.

Zabransky, D.J., Nirschl, C.J., Durham, N.M., Park, B.V., Ceccato, C.M., Bruno, T.C., Tam, A.J., Getnet, D., Drake, C.G., 2012. Phenotypic and functional properties of Helios+ regulatory T cells. PLoS ONE 7, e34547.

Zenclussen, A.C., Gerlof, K., Zenclussen, M.L., Sollwedel, A., Bertoja, A.Z., Ritter, T., Kotsch, K., Leber, J., Volk, H.D., 2005. Abnormal T-cell reactivity against paternal antigens in spontaneous abortion: adoptive transfer of pregnancy-induced CD4+CD25+ T regulatory cells prevents fetal rejection in a murine abortion model. Am. J. Pathol. 166, 811–822.

Zenclussen, A.C., Gerlof, K., Zenclussen, M.L., Ritschel, S., Zambon Bertoja, A., Fest, S., Hontsu, S., Ueha, S., Matsushima, K., Leber, J., Volk, H.D., 2006. Regulatory T cells induce a privileged tolerant microenvironment at the fetal–maternal interface. Eur. J. Immunol. 36, 82–94.

BIOLOGY OF REPRODUCTION (2014) 91(5):129, 1–11
Published online before print 1 October 2014.
DOI 10.1095/biolreprod.114.121616

Human Exosomal Placenta-Associated *miR-517a-3p* Modulates the Expression of *PRKG1* mRNA in Jurkat Cells[1]

Saori Kambe,[3,4] Hiroshi Yoshitake,[3] Kazuya Yuge,[3] Yoichi Ishida,[5] Md. Moksed Ali,[3] Takami Takizawa,[3] Tomoyuki Kuwata,[5] Akihide Ohkuchi,[5] Shigeki Matsubara,[5] Mitsuaki Suzuki,[5] Toshiyuki Takeshita,[4] Shigeru Saito,[6] and Toshihiro Takizawa[2,3]

[3]*Department of Molecular Medicine and Anatomy, Nippon Medical School, Tokyo, Japan*
[4]*Department of Reproductive Medicine, Perinatology and Gynecologic Oncology, Nippon Medical School, Tokyo, Japan*
[5]*Department of Obstetrics and Gynecology, Jichi Medical University, Tochigi, Japan*
[6]*Department of Obstetrics and Gynecology, Faculty of Medicine, University of Toyama, Toyama, Japan*

ABSTRACT

During pregnancy, human placenta-associated microRNAs (miRNAs) derived from the miRNA cluster in human chromosome 19 are expressed in villous trophoblasts and secreted into maternal circulation via exosomes; however, little is known about whether circulating placenta-associated miRNAs are transferred into maternal immune cells via exosomes, and modulate expression of target genes in the recipient cells. We employed an in vitro model of trophoblast-immune cell communication using BeWo cells (a human trophoblast cell line) and Jurkat cells (a human leukemic T-cell line) and investigated whether BeWo exosomal placenta-associated miRNAs can suppress expression of target genes in the recipient Jurkat cells. Using this system, we identified *PRKG1* as a target gene of placenta-associated miRNA *miR-517a-3p*. Moreover, we demonstrated that BeWo exosomal *miR-517a-3p* was internalized into Jurkat cells and subsequently suppressed the expression of *PRKG1* in recipient Jurkat cells. Furthermore, using peripheral blood natural killer (NK) cells in vivo, we confirmed that circulating *miR-517a-3p* was delivered into maternal NK cells as it was into Jurkat cells in vitro. Placenta-associated *miR-517a-3p* was incorporated into maternal NK cells in the third trimester, and it was rapidly cleared after delivery. Expression levels of *miR-517a-3p* and its target mRNA *PRKG1* were inversely correlated in NK cells before and after delivery. These in vitro and in vivo results suggest that exosome-mediated transfer of placenta-associated miRNAs and subsequent modulation of their target genes occur in maternal NK cells. The present study provides novel insight into our understanding of placenta-maternal communication.

BeWo, exosome, human placenta, Jurkat, microRNA, natural killer cell, PRKG1, regulatory T cell, villous trophoblast

[1]Supported by Grants-in-Aid for Scientific Research no. 23390086 to S.S. and no. 24390383 to Toshihiro Takizawa from the Ministry of Education, Culture, Sports, Science and Technology (MEXT), Japan, and by a grant from the MEXT-supported Program for the Strategic Research Foundation at Private Universities (2013–2017) to Toshihiro Takizawa.
[2]Correspondence: Toshihiro Takizawa, Department of Molecular Medicine and Anatomy, Nippon Medical School, 1-1-5 Sendagi, Tokyo 113-8602, Japan. E-mail: t-takizawa@nms.ac.jp

Received: 18 May 2014.
First decision: 12 June 2014.
Accepted: 29 September 2014.

eISSN: 1529-7268 http://www.biolreprod.org
ISSN: 0006-3363

INTRODUCTION

Exosomes are nanovesicles (30–100 nm) of multivesicular body origin that can be released from the cell surface by exocytosis [1]. Most cell types are believed to be able to secrete exosomes [2], which can reach bodily fluids, such as plasma [3], urine [4], semen [5], milk [6], and saliva [7]. To date, it is well known that exosomes contain RNAs, lipids, and many kinds of proteins, which are all thought to transfer from the cell of origin to adjacent or distant cells and influence biological functions of the recipient cells [8, 9]. There has been a growing interest in the role of exosomal microRNAs (miRNAs) in cell-cell communication since Valadi et al. [10] demonstrated that miRNAs exist in exosomes. MicroRNAs are small noncoding RNAs approximately 22 nucleotides in length that play a pivotal role in posttranscriptional gene regulation by repressing target mRNA translation by base pairing to the 3′-untranslated region (3′-UTR) [11, 12]. Recent studies have suggested that exosomes have the capacity to shuttle genetic information from cell to cell by transferring miRNAs [13].

MicroRNAs within the human imprinted chromosome 19 miRNA cluster (C19MC), a primate-specific miRNA cluster encompassing 46 miRNAs in the human genome, are expressed exclusively in the placenta (i.e., placenta-associated miRNAs) [14–16]. Although C19MC-associated miRNAs are not detected in other normal adult tissues, they were also identified in some cancer cells [17]. Recent studies have shown that C19MC-associated miRNAs that are packaged within trophoblast-derived exosomes confer viral resistance in recipient cells by the induction of autophagy [18, 19]. However, the biological functions of C19MC-associated miRNAs for the placenta and pregnancy are still not fully understood. We reported previously that placenta-associated miRNAs are expressed in human villous trophoblasts and are secreted into the maternal circulation via exosomes [20]. Exosomal miRNAs are generally considered to be stable in the circulation [21]. This has raised the possibility that exosomal placenta-associated miRNAs may be detected in the circulation during pregnancy [22, 23] and may serve as novel predictive markers [24]. However, there is little information on how exosomal placenta-associated miRNAs participate in cell-cell communication and possibly contribute to the maintenance of pregnancy.

Based on the aforementioned findings of exosomal miRNAs, we hypothesized that circulating placenta-associated miRNAs might be transferred via exosomes from placental trophoblasts into maternal immune cells and repress expression of target genes in the recipient cells. To test our hypothesis, we initially attempted to search target genes of placenta-associated miRNAs in human peripheral blood immune cells using a DNA microarray analysis. However, this in vivo evaluation proved difficult because these immune cells already contain various miRNAs derived not only from placental cells but also many other cell types [25]. In this study, to avoid the complexity of microarray experiments using circulating cells, we have developed an in vitro model system of trophoblast-immune cell communication using BeWo cells (a human trophoblast cell line) [26] and Jurkat cells (a human leukemic T-cell line) [27]. Using this system, we identified *PRKG1* as a target gene of the placenta-associated miRNA *miR-517a-3p*, via a combination of DNA microarray and in silico analyses. We showed that exosomal *miR-517a-3p* can transfer from BeWo cells into Jurkat cells and modulate the target gene within the recipient cells. Furthermore, we evaluated the uptake of circulating *miR-517a-3p* into immune cells using peripheral blood samples from pregnant women.

MATERIALS AND METHODS

Cell Culture

Jurkat and BeWo cells were purchased from the RIKEN Bioresource Center. JEG3 cells were obtained from the European Collection of Cell Cultures. Jurkat cells were maintained in exosome-free RPMI 1640 medium (Gibco) supplemented with 10% fetal bovine serum (FBS; Japan Bioserum; 37°C, 5% CO_2); BeWo cells were cultured in exosome-free Ham F-12 medium (Invitrogen) supplemented with 15% FBS (37°C, 5% CO_2); JEG-3 was cultured in exosome-free E-MEM (Wako) supplemented with 10% FBS, 1% nonessential amino acids, and 1 mM pyruvate (37°C, 5% CO_2). Exosome-free medium was prepared by ultracentrifugation at 100 000 × *g* for 12 h at 4°C according to the method of Thery et al. [28].

Isolation of Peripheral Blood Immune Cells from Pregnant Women

Samples of peripheral blood were obtained from full-term pregnant women who gave informed consent (n = 24; gestational age, 36–38 wk). Protocols were approved by the ethics committees of Nippon Medical School and Jichi Medical University. Postdelivery maternal blood samples were also collected 4 days after delivery. Women with significant comorbid medical conditions or concomitant medications that would substantially impact immunologic function were excluded from the study. Peripheral blood mononuclear cells (MNCs) were isolated from heparinized venous blood using Lymphoprep (Axis-Shield PoC AS). Briefly, after the blood was centrifuged at 1490 × *g* for 15 min at 4°C, the pellet was resuspended in PBS containing 1% bovine serum albumin (buffer A). The MNCs were isolated from the suspension according to the manufacturer's instructions, and then were resuspended in buffer A. Natural killer (NK) cells and regulatory T (Treg) cells were isolated from the MNCs using Dynabeads Untouched NK-cell and Dynabeads Regulatory $CD4^+CD25^+$ T-cell kits (Invitrogen), respectively, according to the manufacturer's instructions. Total RNA from the cells was extracted as described below.

Exosome Isolation from Culture Supernatants

Exosomes were isolated from the supernatant of trophoblast cell lines according to the method of Thery et al. [28]. Briefly, culture supernatants were harvested and sequentially centrifuged at 4°C at 300 × *g* for 10 min, 2000 × *g* for 10 min, and 10 000 × *g* for 30 min to eliminate cells, dead cells, and cell debris. The supernatants were filtered through a 0.22-μm filter and then ultracentrifuged at 100 000 × *g* for 70 min at 4°C to pellet exosomes. Exosomal pellets were washed twice in PBS and then resuspended in 200 μl of PBS. The protein content of purified exosomes was determined using a BCA protein assay kit (Pierce).

Exosomes were also prepared from culture supernatants of BeWo cells transfected with Pre-miR-517a (mature *miR-517a-3p* mimic; Applied Biosystems), Pre-miR-1, or Pre-miR Negative Control no. 1 (Pre-miR-NC) to investigate the effect of these miRNAs in the recipient Jurkat cells. BeWo cells were transfected with Pre-miR reagents (30 nM) using Lipofectamine 2000 (Invitrogen) for 4 h. After 48 h of transfection, culture supernatants were collected for exosome isolation. Exosomes from Pre-miR-517a-transfected, Pre-miR-1-transfected, and Pre-miR-NC-transfected BeWo cells were designated *miR-517a-3p*-loaded, *miR-1*-loaded, and miR-NC-loaded exosomes, respectively; exosomes from nontransfected cells were designated wild-type exosomes.

RNA Extraction and Purification

Total RNA within whole cells was extracted using RNAiso reagent (Takara), followed by cleanup with RNeasy Mini Kits (Qiagen), according to the manufacturer's instructions. Total RNA within exosomes was extracted using mirVana miRNA Isolation Kits (Applied Biosystems) according to the manufacturer's instructions.

Real-Time PCR Analysis

Real-time PCR for miRNAs was carried out using TaqMan MicroRNA Assays (Applied Biosystems) in a 7300 Real-Time PCR System (Applied Biosystems) or a 7900 FAST Real-Time PCR System (Applied Biosystems). Briefly, total RNA was reverse transcribed with the High Capacity cDNA Reverse Transcription Kit (Applied Biosystems). The RT products were subsequently subjected to a real-time PCR reaction using TaqMan 2X Universal PCR Master Mix (Applied Biosystems). To quantify mRNA levels, SYBR Premix Ex Taq (Takara Bio) was applied. Total RNA was reverse transcribed with PrimeScript RT reagent Kit (Takara). To quantify mRNA levels, SYBR Premix Ex Taq was applied. To normalize expression levels of miRNAs and mRNAs, *SNORD44* and *GAPDH* were used as endogenous internal controls, respectively. Primers for *miR-512-3p* (assay ID 001823), *miR-517a-3p* (assay ID 002402), *miR-518b* (assay ID 001156), and *miR-1* (assay ID 002222) were from Applied Biosystems. Primers for mRNAs (Eurofins Genomics) were as follows: *ALDH1B1*: forward, CCTGGCTGCGGCTGTGTTCA; reverse, ATGGCGTGTGGCAGGTGACG; *ANP32E*: forward, CCCCGGAGGAGGTGACAGAGT; reverse, AGCCGGGC CAGCGAACTTAG; *DHFR*: forward, CTGCATCGTCGCTGTGTCCCA; reverse, ATTCCTGAGCGGTGGCCAGG; *FAT2*: forward, TCCAGAGTGAG GAAGAGGTA; reverse, TGTGGAGAATTGGGGTATAG; *IGSF5*: forward, CTGGACCCGGCTCCCGGATA; reverse, GAAGGTCGCTGGGCTCCGGA; *PRKG1*: forward, AGGAGCTGAGGCAGCGGGAT; reverse, CAAGGTGC TCGCGCTCTGCT; *TWF1*: forward, GGAGGACAAACAACCATGCTA; reverse, GGGAAGATTGTGACAGCAAGT; and *RSPO3*: forward, TCGGCAGC CAAAACGCCTCC; reverse, TGCACAGCCTCCTTGGCAGC.

Western Blot Analysis

Proteins derived from BeWo cells or Jurkat cells were obtained using M-PER Mammalian Protein Extraction Reagent (Thermo Fisher Scientific) containing Halt Protease Inhibitor Cocktail (Thermo Fisher Scientific). Proteins were separated on 10% SDS-PAGE gels and were transferred onto Sequi-blot PVDF membranes (Bio-Rad). Blots were incubated at 4°C overnight with primary antibodies followed by incubation with horseradish peroxidase-conjugated secondary antibodies. Antibodies used in Western blotting were as follows: anti-CD63 monoclonal antibody (mAb; Sanquin), anti-CD81 polyclonal antibody (pAb; Santa Cruz Biotechnology), anti-TSG101 pAb (Sigma-Aldrich), anti-ACTB mAb (Sigma-Aldrich), anti-PRKG1 mAb (Cell Signaling Technologies), and horseradish peroxidase-conjugated secondary antibodies (Pierce). Signals were detected using Immobilon reagent (Millipore) and visualized using an LAS-4000 Lumino image analyzer (Fujifilm).

Immunoelectron Microscopy Analysis

For immunogold labeling of CD63, an mAb (H5C6; provided by Developmental Studies Hybridoma Bank, Department of Biological Sciences, University of Iowa) was employed. Exosomes were fixed with 4% paraformaldehyde (Merck) in PBS, and 20 μl of the suspension was placed on 300-mesh nickel grids (Electron Microscopy Sciences) coated with Formvar (Nisshin EM), for 20 min at 22°C. After blocking with 5% normal goat serum (Sigma-Aldrich) in PBS, grids bearing exosomes were incubated with anti-CD63 for 30 min at 37°C. The grids were then incubated with goat anti-mouse immunoglobulin G (IgG) pAb conjugated to 10-nm colloidal gold particles (Jackson Immunoresearch), for 30 min at 37°C. Immunolabeled exosomes on grids were postfixed with 2% glutaraldehyde in PBS for 30 min at 22°C, and then negatively stained with 4% uranyl acetate according to the method of Sakai et al. [29]. Control grids received the same treatment except that the primary antibody was replaced with nonimmune isotype-matched IgG (MOPC-21; Sigma-Aldrich). Samples were observed under a Hitachi H-7650 electron microscope system (Hitachi High-Technologies) operated at 80 kV.

Morphometric analysis of isolated vesicles in electron micrographs was performed. The size of isolated vesicles was measured, and the number of the vesicles labeled with and without colloidal gold particles indicating CD63 was

counted on the micrographs printed at the same magnification (150 000×). A total of 221 vesicles were analyzed.

Microarray Analysis in miR-517a-3p*–Overexpressing Jurkat Cells*

Jurkat cells were transfected with Pre-miR-517a or Pre-miR NC at a final concentration of 40 nM using Lipofectamine 2000. Pre-miR-transfected cells were harvested 48 h after transfection and total RNA was extracted as described above. The integrity of RNA for microarray analysis was determined using an Agilent 2100 Bioanalyzer (Agilent Technologies); samples with RNA integrity number greater than 7 were used. Of the total RNA obtained, 100 ng was used in a labeling reaction using a Low-Input QuickAmp Labeling Kit, One-Color (Agilent Technologies), and the quality and yield of labeled cRNA were evaluated on an Agilent 2100 Bioanalyzer. Gene expression profiling was conducted using an Agilent microarray (Human GE 4×44 K, v2). The resulting signals were normalized to the 75th percentile signal intensity, and processed data were filtered using a 2-fold change threshold with GeneSpring GX software (v. 11.5; Agilent Technologies). The mRNA array data are publicly available (Gene Expression Omnibus accession no. GSE50814; http://www.ncbi.nlm.nih.gov/geo/; accessed September 12, 2013).

MicroRNA Target Prediction

We focused on downregulated mRNAs as potential direct targets of *miR-517a-3p* in the above DNA microarray analysis. The online prediction software MicroCosm Targets version 5 (http://www.ebi.ac.uk/enright-srv/microcosm/htdocs/targets/v5/; accessed October 1, 2011) was used to search for predicted target genes of *miR-517a-3p*.

Luciferase Assay

To construct a reporter plasmid, we first cloned the 3′-UTR of the human *PRKG1* gene (GenBank accession no. NM_006258) into the pMIR-REPORT vector, in which firefly luciferase expression reports miRNA activity (Applied Biosystems). Genomic DNA from Jurkat cells was isolated using the FastPure DNA Kit (Takara). The 3′-UTR of the *PRKG1* mRNA was then amplified from isolated genomic DNA using the following primers: 5′-CAGG**ACTAGT**TG-TATTTCTCTTACCTGCTTCTGCCT-3′ (*Spe*I site underlined) and 5′-GGCA**AAGCTT**GTTACTTATGACAGCTAATAATAGTCAACTGGC-3′ (*Hin*dIII site underlined). After sequence verification by cloning into a pCR-Blunt II-TOPO vector, the *PRKG1* 3′-UTR was cloned into pMIR-REPORT via the *Spe*I and *Hin*dIII restriction sites. This final construct was designated pMIR-PRKG1. To construct a reporter plasmid with a mutated *miR-517a-3p* recognition site of *PRKG1* 3′-UTR (see Fig. 3D), an inverse PCR method was used. The primers used for the inverse PCR were *PRKG1* 3′-UTR mut forward, 5′-ACAGAagactgaaaaattagtacgtaaATTTGTTTGTTTTTTTTGATAAATTGG CATG-3′; and *PRKG1* 3′-UTR mut reverse, 5′-ACAAATttacgtactaattttt cagtctTCTGTGAAAACTCATATATACCTACTATGAGAGGTCTC-3′ (complementary sequence shown in lowercase), and were designed to introduce the mutation. The PCR amplification was carried out using the previously cloned vector pCR-Blunt II-TOPO containing the *PRKG1* 3′-UTR. Plasmid DNA was digested by *Dpn*I. The final construct was confirmed by sequencing using an ABI PRISM 3130 Genetic Analyzer (Applied Biosystems). Amplified DNA was transformed into *Escherichia coli*. After sequence verification, the mutated 3′-UTR sequence was cloned into pMIR-REPORT via *Spe*I and *Hin*dIII restriction sites. The final construct was designated pMIR-PRKG1mt.

Jurkat cells were transfected with pMIR-PRKG1, pMIR-PRKG1mt, or pMIR-cont (empty vector pMiR-REPORT), and the control vector pRL-TK (*Renilla* luciferase expression plasmid), together with Pre-miR-517a or Pre-miR-NC (30 nM), using Lipofectamine 2000 in 24-well plates. Twenty-four hours after transfection, luciferase assays were performed using the Dual Luciferase Reporter Assay System (Promega). Firefly luciferase activity was normalized to *Renilla* luciferase activity.

Transfer of BeWo Exosomes into Recipient Cells

Jurkat cells were incubated with exosomes isolated from trophoblast cell lines (50 μg/ml) for 24–48 h, and real-time PCR was performed for quantification of miRNA and mRNA as described above. For luciferase assay, Jurkat cells were transfected with pMIR-PRKG1or pMIR-cont, and the control vector pRL-TK. After 24 h of transfection, cells were incubated with BeWo exosomes for another 24 h, and then luciferase assays were performed. Some cells were incubated with BeWo exosomes for 24 h, washed twice with PBS, and then treated with TrypLE Express Enzyme solution (recombinant trypsin-like serine protease [1×] in Dulbecco PBS/1 mM ethylene diamine tetraacetic acid [EDTA]; Gibco) for 10 min at 37°C. The expression levels of *miR-517a-3p* were assayed by real-time PCR.

Isolated peripheral blood immune cells were incubated with BeWo exosomes (50 μg/ml) in exosome-free RPMI 1640 medium supplemented with 10% FBS for 24 h, and the expression levels of *miR-517a-3p* were assayed by real-time PCR.

Statistical Analysis

We conducted all analyses using the SPSS statistical software package (Windows version 20; IBM-SPSS). The significance of between-group differences was assessed using Student *t*-test, ANOVA followed by Tukey test, or Kruskal-Wallis test, and P values <0.05 were considered to indicate statistical significance.

RESULTS

Characterization of Exosomes Derived from BeWo Cells

We first investigated whether BeWo cells could release exosomes into the extracellular space. Because exosomes are known to express CD63, CD81, and TSG101 [3], we examined expression of these molecules in the exosomal fraction isolated from BeWo cell culture medium. As shown in Figure 1A, Western blotting detected all of these molecules in the exosomal fraction, indicating that BeWo cells secrete exosomes into the culture medium. We also confirmed the secretion of exosomes from BeWo cells by immunoelectron microscopy (Fig. 1B). Morphometric analysis of isolated vesicles showed that approximately 80% of the vesicles were positive for CD63. Most of the vesicles were in the 26- to 125-nm range (diameter [mean ± SD], 85 ± 33 nm; Fig. 1C). Moreover, we determined whether the placenta-associated miRNA *miR-517a-3p* exists in exosomes derived from BeWo cells by real-time PCR (Fig. 1D). As expected, *miR-517a-3p* was identified in exosomes secreted from BeWo cells but was not detectable in Jurkat cells.

In Vitro Model of Trophoblast-Immune Cell Communication

To investigate the possibility of functional miRNA transfer from placenta trophoblasts to maternal peripheral blood immune cells via exosomes, we employed an in vitro model system using BeWo and Jurkat cells (Fig. 2A). To confirm whether this system serves as an in vitro model of cell-to-cell communication via exosomes, we first examined transfer of placenta-associated miRNAs to Jurkat cells. Because human placenta expresses placenta-associated miRNAs, such as *miR-512-3p* and *miR-517a-3p*, which are secreted into maternal circulation via exosomes [20, 30], we evaluated the presence of these miRNAs in Jurkat cells after incubation with exosomes released from trophoblast cell lines (BeWo and JEG3 cells) by real-time PCR. When Jurkat cells were incubated with BeWo or JEG3 exosomes for 24 h, *miR-512-3p* and *miR-517a-3p* were detected in the cells (Fig. 2B). In contrast, these miRNAs were not detectable in Jurkat cells treated without exosomes (vehicle). It is likely that miRNAs were transferred into Jurkat cells via trophoblast cell line exosomes.

Target Identification of Placenta-Associated miRNA miR-517a-3p *in Jurkat Cells*

As shown in Figure 2A, a BeWo exosomal miRNA would be expected to bind to a partially complementary sequence (seed sequence) in the 3′-UTR of its target mRNA and suppress translation in recipient Jurkat cells. We next investigated whether BeWo-derived placenta-associated miRNAs function as posttranscriptional gene regulators within

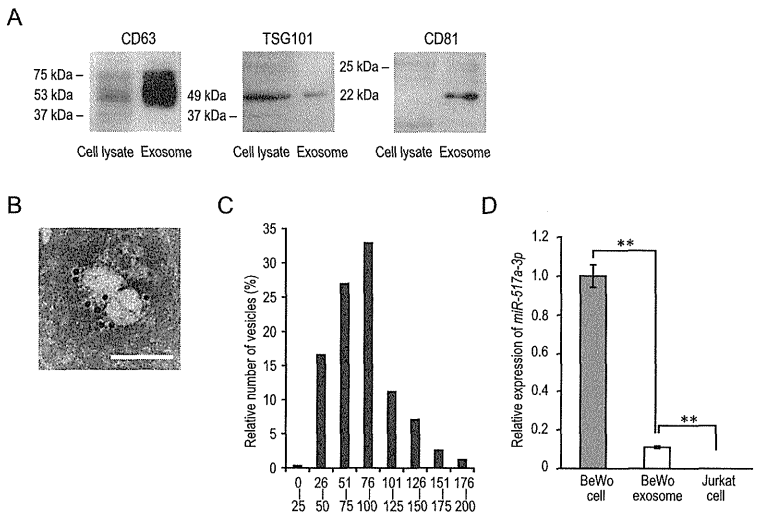

FIG. 1. Characterization of exosomes isolated from culture supernatants of BeWo cells. **A**) Western blots for exosome markers (CD63, CD81, and TSG101) in BeWo cell lysates (Cell lysate) and exosomal pellets collected from culture supernatants (Exosome). **B**) Immunoelectron microscopy of BeWo exosomal pellets. Negatively stained exosomes are labeled with 10-nm colloidal gold particles recognizing CD63. Bar = 100 μm. **C**) Histogram of the number of isolated BeWo vesicles' diameters. The *y* axis shows the relative number of vesicles (%), and the *x* axis shows the vesicle diameter (nm). Vesicles were sorted into 25-nm bins. **D**) Real-time PCR analysis of *miR-517a-3p* expression in BeWo cells, wild-type exosomes derived from the same cells, and Jurkat cells. Data were normalized to *SNORD44*. Expression in BeWo cells was defined as 1. Data are means ± SD of the results from three independent experiments. Tukey test; $^{**}P < 0.01$.

Jurkat cells after exosome-mediated miRNA transfer. For this purpose, we initially identified candidate target mRNAs of the placenta-associated miRNAs using DNA microarray analysis. In this examination, we focused on *miR-517a-3p* as a representative exosomal placenta-associated miRNA, because this miRNA was detected at high levels in the plasma of pregnant women [20] and in isolated human trophoblast cells [30, 31]. Transfection of Jurkat cells with Pre-miR-517a significantly downregulated 123 genes (Supplemental Table S1, available online at www.biolreprod.org). Among the 123 genes identified, we searched for potential direct targets of *miR-517a-3p* using the online software MicroCosm Targets. Seven genes, *ALDH1B1*, *ANP32E*, *DHFR*, *FAT2*, *IGSF5*, *PRKG1*, and *RSPO3*, had at least one potential *miR-517a-3p*-binding site in their 3′-UTRs.

To confirm downregulated expression of these seven genes, we performed real-time PCR. Among the seven mRNAs selected, *PRKG1* was significantly downregulated in *miR-517a-3p*-overexpressing Jurkat cells (Fig. 3A), whereas expression of *ALDH1B1*, *ANP32E*, *DHFR*, *FAT2*, and *RSPO3* was not significantly altered (data not shown). *IGSF5* expression was undetectable (data not shown). As shown in Figure 3B, PRKG1 protein expression was markedly decreased in Pre-miR-517a-transfected cells compared with control cells. Therefore, we focused on *PRKG1* for *miR-517a-3p* target validation.

We used a luciferase assay to determine whether *PRKG1* is a direct target of *miR-517a-3p*. Overexpression of *miR-517a-3p* significantly decreased luciferase activity in Jurkat cells cotransfected with pMIR-PRKG1 (49% reduction compared with the negative control), but not significantly in cells cotransfected with pMIR-PRKG1mt (Fig. 3C), a reporter plasmid in which the putative *miR-517a-3p* recognition site in the *PRKG1* 3′-UTR is mutated (Fig. 3D). Taken together, these results suggest that *PRKG1* is a target of *miR-517a-3p* in Jurkat cells.

Effect of BeWo Exosomal miR-517a-3p *on* PRKG1 *Expression in Jurkat Cells*

We further investigated whether BeWo exosomal *miR-517a-3p* can modulate *PRKG1* mRNA expression within recipient Jurkat cells. In this examination, we also used *miR-517a-3p*-loaded exosomes collected from culture supernatants of BeWo cells transfected with Pre-miR-517a to enhance the effect of this miRNA in the recipient Jurkat cells because we could not generate C19MC *mir-517a* gene-knockout BeWo cells. As shown in Figure 4A, levels of *miR-517a-3p* were greatly increased in the exosome fraction of cell culture supernatants from Pre-miR-517a-transfected BeWo cells (more than 30-fold greater than that from nontransfected cells).

We quantified exosomal *miR-517a-3p* in Jurkat cells incubated with BeWo exosomes. *miR-517a-3p* was not

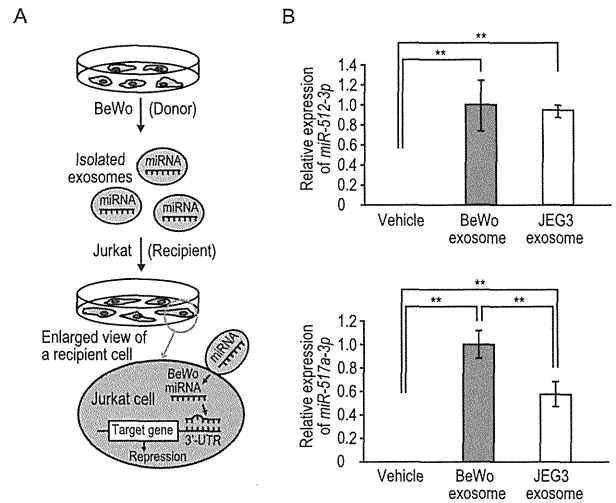

FIG. 2. In vitro model system of trophoblast-immune cell communication. **A**) Scheme of the in vitro transfer system using BeWo cells as donors and Jurkat cells as recipients. Exosomes were collected from culture supernatants of BeWo cells. BeWo exosomes carrying placenta-associated miRNAs (e.g., *miR-517a-3p*) were then added to Jurkat cell culture medium. BeWo exosomal miRNAs were then transferred into Jurkat cells, where they bind to the 3′-UTRs of target genes. **B**) Detection of placenta-associated miRNAs in Jurkat cells treated with wild-type exosomes derived from trophoblast cell lines, BeWo cells, and JEG3 cells. Jurkat cells were incubated in the presence or absence (Vehicle) of exosomes (50 μg/ml) for 24 h. Expression of placenta-associated miRNAs (*miR-512-3p* and *miR-517a-3p*) was analyzed by real-time PCR. Data were normalized to *SNORD44*. Expression in Jurkat cells incubated with BeWo exosomes was defined as 1. Data are means ± SD of the results from three independent experiments. Tukey test; $^{**}P < 0.01$.

detected in Jurkat cells incubated without BeWo cell exosomes (vehicle), and *miR-517a-3p* levels were increased significantly in Jurkat cells treated with BeWo wild-type exosomes (Fig. 4B). Moreover, when Jurkat cells were treated with BeWo *miR-517a-3p*-loaded exosomes, markedly greater levels of *miR-517a-3p* levels were transferred to recipient cells compared with treatment with wild-type exosomes (Fig. 4B). We then investigated whether transferred exosomal *miR-517a-3p* represses endogenous *PRKG1* expression in Jurkat cells. As expected, the expression levels of *PRKG1* were slightly but significantly decreased in Jurkat cells incubated with wild-type exosomes (42% reduction) compared with vehicle-treated cells (Fig. 4C). Further, downregulation of *PRKG1* expression was significantly enhanced by treatment with *miR-517a-3p*-loaded exosomes (70% reduction) compared with vehicle-treated cells (Fig. 4C). In addition, we measured exosomal *miR-517a-3p* in Jurkat cells incubated with BeWo miR-NC-loaded exosomes. No differences were found in the expression levels of *miR-517a-3p* and *PRKG1* between cells treated with miR-NC-loaded exosomes and wild-type exosomes (data not shown).

We also confirmed that exosomal *miR-517a-3p* bound to the 3′-UTR of *PRKG1* in recipient cells by luciferase assay. In pMIR-PRKG1-transfected Jurkat cells, BeWo wild-type exosomes significantly reduced luciferase activity (31% reduction) compared with pMIR-cont-transfected cells; downregulation of *PRKG1* expression was enhanced by incubation with *miR-517a-3p*-loaded exosomes (51% reduction) compared with pMIR-cont-transfected cells (Fig. 4D). Furthermore, we investigated whether remaining cell surface-bound BeWo exosomes affect the expression levels of *miR-517a-3p* that was transferred to Jurkat cells. Jurkat cells were incubated with BeWo exosomes for 24 h, followed by TrypLE digestion (recombinant trypsin-like serine protease-EDTA). These were no differences in the miRNA expression levels between *miR-517a-3p* recipient cells treated with and without TrypLE (Fig. 4E). These results show that BeWo exosomal miRNA *miR-517a-3p* internalized into Jurkat cells and subsequently repressed expression of the target gene *PRKG1* therein.

We used *miR-517a-3p*-loaded exosomes for assessment of the effect of BeWo exosomal *miR-517a-3p* on *PRKG1* in Jurkat cells. An *miR-1* transfection and *TWF1* detection system [32] was also employed to demonstrate that BeWo exosomal miRNAs can transfer to Jurkat cells and suppress target genes in the recipient cells. *TWF1* mRNA is a validated target of *miR-1*, and the repression occurs at the mRNA level [33]. When BeWo *miR-1*-loaded exosomes were incubated with Jurkat cells, *miR-1* was significantly detected in the recipient cells (Fig. 4F). In contrast, *miR-1* was undetectable in Jurkat cells treated with BeWo miR-NC-loaded exosomes (Fig, 4F). As expected, the *miR-1* recipent cells displayed a 55% knockdown of *TWF1* mRNA compared with the miR-NC recipient cells (Fig. 4G). The inverse relationship between *miR-1* expression and the expression level of *TWF1* mRNA provided additional data supporting that BeWo exosomal miRNAs can transfer to Jurkat cells and suppress target genes in the recipient cells.

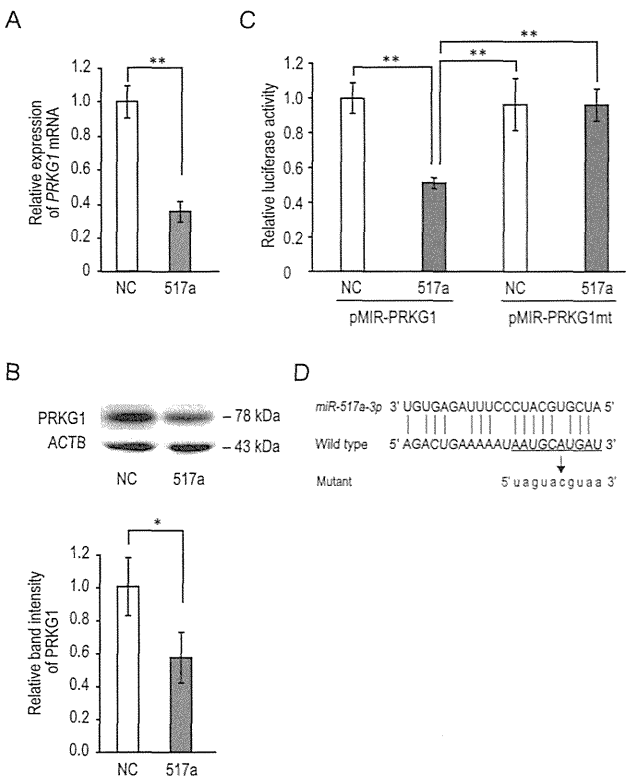

FIG. 3. Validation of *PRKG1* as a *miR-517a-3p* target. **A**) Real-time PCR analysis of candidate *miR-517a-3p* target mRNA *PRKG1* in Jurkat cells. Jurkat cells were transfected with Pre-miR-517a (517a) or Pre-miR-NC (NC), each 40 nM, and cultured for 48 h. Expression of *PRKG1* was examined by real-time PCR. Data were normalized to *GAPDH*. Expression in cells treated with Pre-miR-NC was defined as 1. **B**) Western blots for PRKG1 in Jurkat cells transfected with Pre-miR-517a or Pre-miR-NC (30 μg of total protein per lane). ACTB served as the internal control. Analysis of band intensity is presented as the relative ratio of PRKG1 to ACTB. The relative ratio of PRKG1 in cells treated with Pre-miR-NC was defined as 1. **C**) *PRKG1* 3′-UTR luciferase reporter assay. Reporter vector (pMIR-RPKG1 or pMIR-PRKG1mt) and Pre-miRNA (Pre-miR-517a or Pre-miR-NC [each 30 nM]) were cotransfected into Jurkat cells. *Renilla* luciferase vector pRL-TK was used as the internal control. Luciferase expression levels in cells cotransfected with pMIR-RPKG1 and Pre-miR-NC were defined as 1. **D**) Sequences of mature *miR-517a-3p*, its putative target site in the 3′-UTR of *PRKG1*, and the mutation introduced into the *miR-517a-3p* recognition site of *PRKG1* 3′-UTR in the reporter plasmid. Data are means ± SD of the results from three independent experiments. Student *t*-test (**A** and **B**) or Tukey test (**C**); $^{*}P < 0.05$, $^{**}P < 0.01$.

Detection of Placenta-Associated miRNA miR-517a-3p *in Maternal Immune Cells Isolated from Peripheral Blood of Full-Term Pregnant Women*

As mentioned above, placenta-associated miRNAs are detectable in the maternal circulation during pregnancy [20, 22, 23]. We next investigated whether these miRNAs in the maternal circulation are delivered into immune cells in peripheral blood as they are into Jurkat cells in vitro. For this purpose, we examined whether *miR-517a-3p* and *miR-518b* are present in immune cells isolated from maternal peripheral blood using real-time PCR. These placenta-associated miRNAs

FIG. 4. Transfer of miRNAs into Jurkat cells via BeWo exosomes. **A**) Real-time PCR analysis of *miR-517a-3p* in BeWo wild-type exosomes (Wt-Ex) and *miR-517a-3p*-loaded exosomes (517a-Ex); expression in Wt-Ex was defined as 1. **B**) Detection of transferred *miR-517a-3p* in Jurkat cells cultured with BeWo exosomes. Jurkat cells were treated with vehicle, Wt-Ex, or 517a-Ex (each 50 μg/ml) for 48 h at 37°C. Expression was analyzed by real-time PCR; data were normalized to *SNORD44*. Expression in Jurkat cells incubated with Wt-Ex was defined as 1. **C**) *PRKG1* silencing by exosomal *miR-517a-3p*

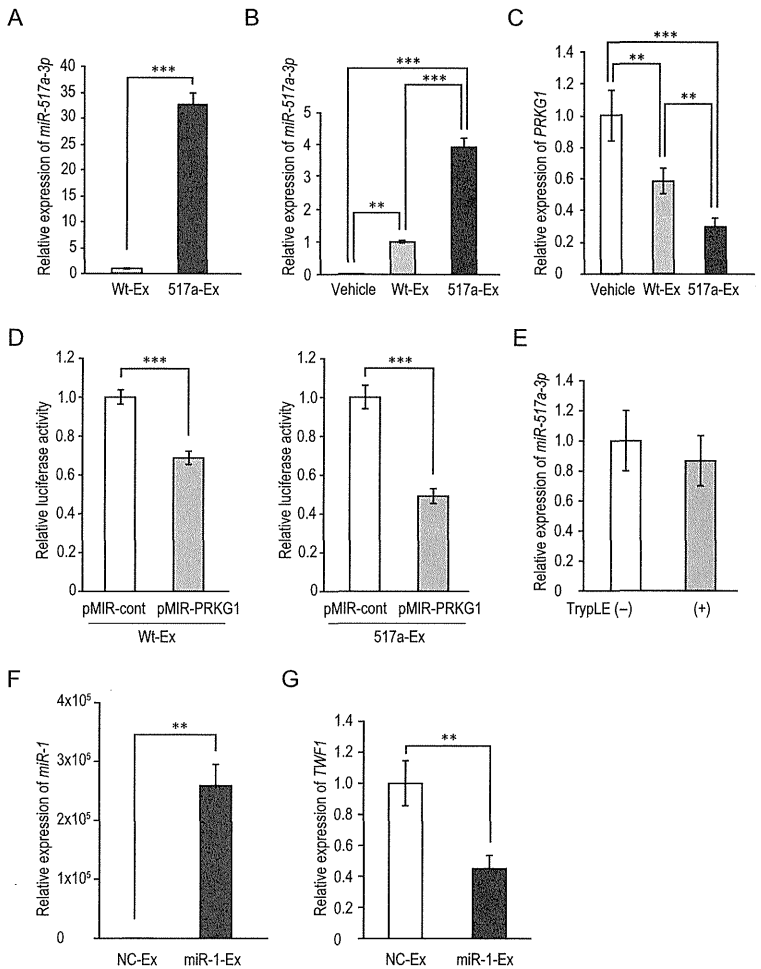

transferred into Jurkat cells. Expression of *PRKG1* in Jurkat cells cultured with vehicle, Wt-Ex, or 517a-Ex for 48 h was evaluated by real-time PCR. Data were normalized to *GAPDH*. Expression in Jurkat cells incubated without exosomes (Vehicle) was defined as 1. **D**) *PRKG1* 3′-UTR luciferase reporter assay in Jurkat cells treated with BeWo exosomes. Jurkat cells transfected with pMIR-cont or pMIR-PRKG1 were incubated with Wt-Ex or 517a-Ex (each 50 μg/ml) for 48 h at 37°C. Luciferase activity in cells transfected with pMIR-cont was defined as 1. **E**) TrypLE digestion of Jurkat cells after incubation with BeWo exosomes. Jurkat cells were incubated with BeWo exosomes (Wt-Ex) for 24 h and then treated with (+) or without (–) TrypLE. Expression of *miR-517a-3p* in Jurkat cells was evaluated by real-time PCR. Data were normalized to *SNORD44*. Expression in cells without TrypLE treatment was defined as 1. **F**) Real-time PCR analysis of *miR-1* in Jurkat cells incubated with BeWo exosomes. Jurkat cells were treated with Pre-miR-NC-loaded exosomes (NC-Ex) or Pre-miR-1-loaded exosomes (1-Ex), each 50 μg/ml, for 24 h at 37°C. Data were normalized to *SNORD44*. Expression in Jurkat cells incubated with NC-Ex was defined as 1. **G**) *TWF1* silencing by exosomal *miR-1* transferred into Jurkat cells. Expression of *TWF1* in Jurkat cells cultured with NC-Ex or 1-Ex for 24 h was evaluated by real-time PCR. Data were normalized to *GAPDH*. Expression in Jurkat cells incubated with NC-Ex was defined as 1. Data are means ± SD from three (**A–D**, **F**, and **G**) and six (**E**) independent examinations. Student *t*-test (**A**, **D–G**) or Tukey test (**B** and **C**); $^{**}P < 0.01$, $^{***}P < 0.001$.

were detected in maternal MNCs before delivery (data not shown). Furthermore, we evaluated the expression of *miR-517a-3p* and *miR-518b* in maternal NK and Treg cells (Fig. 5, A and B) because these cell types play important roles in the maintenance of pregnancy [34, 35]. In NK cells, abundant *miR-517a-3p* and *miR-518b* were detected before delivery; the levels of these miRNAs were significantly reduced at 4 days after delivery (Fig. 5, A and B). In contrast, negligible levels of *miR-517a-3p* and *miR-518b* were detected in Treg cells even before delivery; no differences were found in miRNA levels between before and after delivery (Fig. 5, A and B). In addition, *miR-517a-3p* and *miR-518b* were undetectable in NK and Treg cells from women with no history of pregnancy (Fig. 5, A and B). We also investigated whether expression of *PRKG1* mRNA in maternal NK and Treg cells changes after delivery. As shown in Figure 5C, expression of *PRKG1* in maternal NK cells was significantly upregulated at 4 days after delivery. In maternal Treg cells, the change of *PRKG1* levels was not significant (Fig. 5C). Expression levels of transferred exosomal *miR-517a-3p* and its target *PRKG1*mRNA were inversely correlated and were dependent on pregnancy status, supporting the above-mentioned hypothesis that placental exosomal miRNAs modulate the expression of target genes in maternal immune cells.

To determine whether the uptake of placenta-associated miRNA *miR-517a-3p* into maternal immune cells is dependent on exosomes, we employed an in vitro cell-cell communication model, this time employing male NK and Treg cells instead of Jurkat cells. A significant increase in *miR-517a-3p* levels was detected in NK cells treated with BeWo wild-type exosomes compared with NK cells incubated without BeWo exosomes (Fig. 5D), providing direct evidence that BeWo exosomes can deliver *miR-517a-3p* to NK cells. Unlike maternal Treg cells, exosome-mediated uptake of *miR-517a-3p* into Treg cells was observed in this in vitro model system; however, lower levels of *miR-517a-3p* were transferred into Treg cells than into NK cells (Fig. 5D).

DISCUSSION

Until recently, intercellular communication had been thought to be take place only through cell-to-cell adhesion conduits or secreted signals, such as hormones, cytokines, and neurotransmitters. In addition to these, exosomal RNAs and proteins have been shown to play an important role in intercellular communication [10, 36, 37]. During pregnancy, exosomes are involved in cell-to-cell communication between the placenta and peripheral blood immune cells. For example, Taylor et al. [38], Sabapatha et al. [39], and Atay et al. [40] reported that placenta-derived exosomes exist in the maternal circulation and suppress T-cell signaling components. However, these functional studies measured placental exosome-associated proteins, such as Fas ligand, MHC class I chain-related proteins, and fibronectin. Although it is likely that exosomal C19MC miRNAs contribute to placental-maternal communication, few studies have examined whether exosomal placenta-associated miRNAs modulate the expression of their targets in recipient maternal immune cells.

In the present study, we investigated the possible involvement of exosomal placenta-associated miRNAs in communication between trophoblasts and immune cells using in vitro and in vivo approaches. First, we employed an in vitro model system. We attempted to search target genes of placenta-associated miRNA *miR-517a-3p* using an in vitro trophoblast (BeWo)-immune cell (Jurkat) model system because little has been reported on experimentally validated targets of *miR-517a-3p*. In the present study, we identified *PRKG1* as a target gene of the placenta-associated *miR-517a-3p* (Fig. 3) and demonstrated that BeWo exosomal *miR-517a-3p* was transferable to Jurkat cells and suppressed the expression of *PRKG1* mRNA within the recipient cells (Fig. 4). Next, using maternal peripheral blood cells as an in vivo approach, we confirmed that *miR-517a-3p* in the maternal circulation was delivered into NK cells in peripheral blood as it was into Jurkat cells in vitro. We revealed a negative correlation between the expression levels of transferred exosomal *miR-517a-3p* and its target mRNA *PRKG1* in maternal NK cells before and after delivery (Fig. 5, A and C). In addition, we presented that *miR-517a-3p* was transferred into NK cells via BeWo exosomes (Fig. 5D). These in vivo and in vitro results suggest that exosome-mediated transfer of placenta-associated miRNAs and subsequent modulation of their target genes occur in maternal NK cells during pregnancy.

PRKG1 is a serine/threonine kinase that acts as a key mediator of the nitric oxide (NO)/cGMP signaling pathway [41, 42]. PRKG1 plays a central role in regulating cardiovascular and neuronal functions in addition to relaxing smooth muscle tone, preventing platelet aggregation, and modulating cell growth. In mammals, PRKG1 is strongly expressed in smooth muscle, platelets, cerebellum, hippocampus, dorsal root ganglia, the end plates of neuromuscular junctions, and kidney [43, 44]. In terms of PRKG1 in immune cells, Fischer et al. [45] reported that the NO/cGMP/PRKG1 signaling system negatively regulates T-cell activation and proliferation. Although the biological function of PRKG1 in NK cells is unclear, our present data together with previous findings suggest that *miR-517a-3p* is involved in regulating the activation and proliferation of maternal immune cells by inhibiting NO/cGMP/PRKG1 signaling.

Placenta-associated miRNAs were reduced in maternal NK cells rapidly after delivery (Fig. 5, A and B). What mechanism is involved in this rapid clearance of placenta-associated miRNAs in NK cells? There are some possible explanations for rapid turnover dynamics of placenta-associated miRNAs in NK cells. First, it is possible that the supply of placenta exosomes, including placenta-associated miRNAs, is stopped after a termination of pregnancy. Another explanation may be that rapid degradation of miRNAs occurs in NK cells. Because placenta-associated miRNA levels in maternal plasma decreased dramatically after delivery [20], it seems likely that the halt of the supply of placenta exosomes affects rapid clearance of placenta-associated miRNAs rather than miRNA turnover in NK cells.

Natural killer cells are well known to play important roles in the maintenance of human pregnancy [34]. Although we identified one target gene of *miR-517a-3p* using the in vitro model system used in this study, we could not find other target genes that are associated with immune tolerance in pregnancy. A single miRNA targets multiple mRNAs, and a single mRNA is regulated by multiple miRNAs. This relationship between miRNAs and target genes makes it difficult to study the functional roles of miRNAs. Recently, Olarerin-George et al. [46] have shown *miR-517a-3p* to be a potent activator of nuclear factor-kappa B signaling. Nuclear factor-kappa B plays pivotal roles in immune response [47]. Further identification of targets of these miRNAs and studies of their functions are warranted to comprehensively understand the precise mechanisms by which placental exosomal miRNA-mediated modulation of maternal NK cells contributes to fetomaternal immunotolerance during pregnancy.

The specificity of the exosome-mediated communication between trophoblasts and immune cells remains to be